NASA Contractor Report 2865

A Generalized Vortex Lattice Method for Subsonic and Supersonic Flow Applications

Luis R. Miranda, Robert D. Elliott,
and William M. Baker

Lockheed-California Company
Burbank, California

Prepared for
Langley Research Center
under Contract NAS1-12972

National Aeronautics
and Space Administration

**Scientific and Technical
Information Office**

1977

TABLE OF CONTENTS

LIST OF ILLUSTRATIONS

A GENERALIZED VORTEX LATTICE METHOD FOR SUBSONIC AND SUPERSONIC FLOW APPLICATIONS

Luis R. Miranda, Robert D. Elliott, and William M. Baker
Lockheed-California Company

SUMMARY

A vortex lattice method applicable to both subsonic and supersonic flow is described. It is shown that if the discrete vortex lattice is considered as an approximation to the surface-distributed vorticity, then the concept of the generalized principal part of an integral yields a residual term to the vorticity-induced velocity field. The proper incorporation of this term to the velocity field generated by the discrete vortex lines renders the present vortex lattice method valid for supersonic flow. Special techniques for simulating nonzero thickness lifting surfaces and fusiform bodies with vortex lattice elements are included. Thickness effects of wing-like components are simulated by a double (biplanar) vortex lattice layer, and fusiform bodies are represented by a vortex grid arranged on a series of concentrical cylindrical surfaces. The analysis of sideslip effects by the subject method is described. Numerical considerations peculiar to the application of these techniques are also discussed. A summary comparison of the results obtained by the method of this report with other theoretical and experimental results is presented. This method has been implemented in a digital computer code identified as VORLAX. A users manual for the VORLAX program is contained in Appendix A. A complete Fortran compilation and executed case are contained in Appendix B. Appendices C and D describe input conversion programs useful for transforming input between the VORLAX and NASA Wave Drag programs.

INTRODUCTION

The several versions or variations of the vortex lattice method that are presently available have proven to be very practical and versatile theoretical tools for the aerodynamic analysis and design of planar and nonplanar configurations. The success of the method is due in great part to the relative simplicity of the numerical techniques involved, and to the high accuracy, within the limitations of the basic theory, of the results obtained. But most of the work on vortex lattice methods appears to have concentrated on subsonic flow application. The applicability of the basic techniques of vortex lattice theory to supersonic flow has been largely ignored. The method presented herein allows the direct extension of vortex lattice techniques to supersonic Mach numbers. The equations allowing this extended application are derived in the next section starting from the first order vector equations governing inviscid compressible flow. They are then applied to the particular case of a skewed-horseshoe vortex with special attention given to the supersonic horseshoe.

In the following theoretical discussion, the basic arguments involved in the simulation of thickness and volume effects by vortex lattice elements are presented. This particular modeling of the above effects represents an alternative, with somewhat reduced computational requirements, to the method of quadrilateral vortex rings (refs. 1 and 2). The simulation of thickness and volume effects makes possible the computation of the surface pressure distribution on wing-body configurations. The fact that this can be done without having to resort to additional types of singularities, such as sources, results in a simpler digital computer code.

THEORETICAL DISCUSSION

The Basic Equations

Ward has shown, (ref. 3), that the small-perturbation, linearized flow of an inviscid compressible fluid is governed by the three first order vector equations:

$$\nabla \times \bar{v} = \bar{\omega}, \qquad \nabla . \bar{w} = Q, \qquad \bar{w} = \Psi . \bar{v} \tag{1}$$

on the assumption that the vorticity $\bar{\omega}$ and the source intensity Q are known functions of the point whose position vector is $\bar{R}$. The vector $\bar{v}$ is the perturbation velocity with orthogonal Cartesian components u, v, and w, and Ψ is a constant symmetrical tensor that for orthogonal Cartesian coordinates with the x-axis aligned with the freestream direction has the form

$$\Psi = \begin{bmatrix} 1 - M_\infty^2 & 0 & 0 \\ 0 & 1 & 0 \\ 0 & 0 & 1 \end{bmatrix} \tag{2}$$

where M_∞ is the freestream Mach number. If $\beta^2 = 1-M_\infty^2$, then the vector $\bar{w}$ has the components $\bar{w} = \beta^2 u \bar{i} + v \bar{j} + w \bar{k}$. This vector was first introduced by Robinson (ref. 4), who called it the "reduced current velocity". If $\bar{u}$ denotes the total velocity vector, i.e., $\bar{u} = (u_\infty + u) \bar{i} + v \bar{j} + w \bar{k}$, and ρ the fluid density, then it can be shown that for irrotational and homentropic flow

$$\rho \bar{u} = \rho_\infty \bar{u}_\infty + \rho_\infty \bar{w} + \text{higher order terms} \tag{3}$$

where the subscript ∞ indicates the value of the quantity at upstream infinity, e.g., $\bar{u}_\infty = u_\infty \bar{i}$. Therefore, to a linear approximation, the vector $\bar{w}$ is directly related to the perturbation mass flux as follows:

$$\bar{w} = (\rho \bar{u} - \rho_\infty \bar{u}_\infty) / \rho_\infty \tag{4}$$

The second equation of (1), i.e., the continuity condition, shows that for source-free flows ($Q = 0$), w is a conserved quantity.

Ward has integrated the three first order vector equations directly without having to resort to an auxiliary potential function. He obtained two different solutions for $\bar{v}(\bar{R})$, depending on whether β^2 is positive (subsonic flow), or negative (supersonic flow). These two solutions can be combined formally into a single expression if the following convention is used:

$$K = 2 \quad \text{for} \quad \beta^2 > 0$$

$$K = 1 \quad \text{for} \quad \beta^2 < 0$$

$$R_\beta = \text{Real part of } \left\{ (x-x_1)^2 + \beta^2 \left[(y-y_1)^2 + (z-z_1)^2 \right] \right\}^{1/2}$$

$\int\!\!\!\!\!\!-$ = Finite part of integral as defined by Hadamard (refs. 5 and 6).

The resulting solution for the perturbation velocity $\bar{v}$ at the point whose position vector is $\bar{R}_1 = x_1\,\bar{i} + y_1\,\bar{j} + z_1\,\bar{k}$, is given by

$$\bar{v}(\bar{R}_1) = -\frac{1}{2\pi K} \int\!\!\!\!\!\!-_S \bar{n} \cdot \bar{w}(\bar{R})\, \nabla \frac{1}{R_\beta}\, dS$$

$$+ \frac{\beta^2}{2\pi K} \int\!\!\!\!\!\!-_S \{\bar{n} \times \bar{v}(\bar{R})\} \times \frac{\bar{R} - \bar{R}_1}{R_\beta^3}\, dS$$

$$+ \frac{1}{2\pi K} \int\!\!\!\!\!\!-_V Q(\bar{R})\, \nabla \frac{1}{R_\beta}\, dV + \frac{\beta^2}{2\pi K} \int\!\!\!\!\!\!-_V \frac{\bar{R}-\bar{R}_1}{R_\beta^3} \times \bar{\omega}(\bar{R})\, dV \qquad (5)$$

This formula determines the value of $\bar{v}$ within the region V bounded by the surface S. The vector $\bar{n}$ is the unit outward (from the region V) normal to the surface S. Furthermore, it is understood that for supersonic flow only those parts of V and S lying within the domain of dependence (Mach forecone) of the point $\bar{R}_1$ are to be included in the integration.

For source-free ($Q \equiv 0$), irrotational ($\bar{\omega} \equiv 0$) flow, equation (5) reduces to

$$\bar{v}(\bar{R}_1) = -\frac{1}{2\pi K} \int\!\!\!\!\!\!-_S \bar{n} \cdot \bar{w}(\bar{R})\, \nabla \frac{1}{R_\beta}\, dS + \frac{\beta^2}{2\pi K} \int\!\!\!\!\!\!-_S \{\bar{n} \times \bar{w}(\bar{R})\} \times \frac{\bar{R}-\bar{R}_1}{R_\beta^3}\, dS \qquad (6)$$

This is a relation between $\bar{v}$ inside S and the values of $\bar{n}\cdot\bar{w}$ and $\bar{n} \times \bar{v}$ on S, but these two quantities cannot be specified independently on S.

To determine the source-free, irrotational flow about an arbitrary body B by means of equation (6), assume that the surface S coincides with the wetted surface of the body, with any trailing wake that it may have, and with a sphere of infinite radius enclosing the body and the whole flow field about it, namely, $S = S_B + S_W + S_\infty$.

This surface S divides the space into two regions, V_e external to the body, and V_i internal to it. Applying equation (6) to both V_e and V_i, since the integrals over S_∞ converge to zero, the following expression is obtained:

$$\bar{v}(\bar{R}_1) = \frac{1}{2\pi K} \oint_{S_B + S_W} \bar{N} \cdot \Delta \bar{w}\,(\bar{R})\, \nabla \frac{1}{R_\beta}\, dS - \frac{\beta^2}{2\pi K} \oint_{S_B + S_W} \{\bar{N} \times \Delta \bar{v}(\bar{R})\} \times \frac{\bar{R}-\bar{R}_1}{R^3_\beta}\, dS \quad (7)$$

where $\bar{N} = \bar{n}_i = -\bar{n}_e$ is the unit normal to the body, or wake as the case may be, positive from the interior to the exterior of the body, $\Delta \bar{w} = \bar{w}_e - \bar{w}_i$, and $\Delta \bar{v} = \bar{v}_e - \bar{v}_i$. Here the subscripts designate the values of the quantities on the corresponding face of S. The first surface integral can be considered as representing the contribution of a source distribution of surface density $\bar{N} \cdot \Delta \bar{w}$, while the second surface integral gives the contribution of a vorticity distribution of surface density $\bar{N} \times \Delta \bar{v}$.

If the boundary condition of zero mass flux through the surface $S_B + S_W$ is applied to both external and internal flows

$$\bar{N} \cdot \rho \bar{u}_e = \bar{N} \cdot (\rho_\infty \bar{u}_\infty + \rho_\infty \bar{w}_e) = 0$$
$$\bar{N} \cdot \rho \bar{u}_i = \bar{N} \cdot (\rho_\infty \bar{u}_\infty + \rho_\infty \bar{w}_i) = 0 \quad (8)$$

then the condition $\bar{N} \cdot \Delta \bar{w} = 0$ exists over $S_B + S_W$, and the flow field is uniquely determined by

$$\bar{v}(\bar{R}_1) = -\frac{\beta^2}{2\pi K} \oint_{S_B + S_W} \bar{\gamma}\,(\bar{R}) \times \frac{\bar{R}-\bar{R}_1}{R^3_\beta}\, dS \quad (9)$$

where $\bar{\gamma}\,(\bar{R}) = \bar{N} \times \Delta \bar{v}$ is the surface vorticity density.

Extension to Supersonic Flow

In order to extend the application of the vortex lattice method to supersonic flow, it is essential to consider the fundamental element of the method, the vortex filament, as a numerical approximation scheme to the integral expression (9) instead of a real physical entity. The velocity field generated by a vortex filament can be obtained by a straightforward limiting process, the result being

$$\bar{v}(\bar{R}_1) = \frac{-\beta^2}{2\pi K} \oint_C \bar{\Gamma} \times \frac{\bar{R}-\bar{R}_1}{R^3_\beta}\, d\ell \quad (10)$$

where $\bar{\Gamma} = \lim_{\substack{\bar{\gamma} \to \infty \\ \delta \to 0}} \bar{\gamma} \cdot \delta$

δ is a dimension normal to γ, and $d\ell$ is the distance element along γ. In the classical vortex lattice method, applicable only to subsonic flow, the vorticity distribution over the body and the wake, i.e., over the surface $S_B + S_W$, is replaced by a suitable arrangement of vortex filaments whose velocity fields are everywhere determined by equation (10). This procedure is no longer appropriate for supersonic flow. For this latter case, it is necessary to go back to equation (9) and to derive an approximation to it. This is done in the following.

If the surface $S_B + S_W$, which defines the body and its wake, is considered as being composed of a large number of discrete flat area elements τ over which the surface vorticity density $\bar{\gamma}$ can be assumed approximately constant, then equation (9) can be approximated by the following equation:

$$\bar{v}(\bar{R}_1) = -\frac{\beta^2}{2\pi K} \sum_{J=1}^{N} \oint_{\tau_J} \bar{\gamma}_J \times \frac{\bar{R}-\bar{R}_1}{R^3_\beta} \, dS \qquad (11)$$

where N is the total number of discrete area elements τ. When the point whose position vector is $\bar{R}_1$ is not part of τ_J, the integral over this discrete area can be approximated by the mean value theorem as follows:

$$\oint_{\tau_J} \bar{\gamma}_J \times \frac{\bar{R}-\bar{R}_1}{R^3_\beta} \, dS = \bar{\gamma}_J \, \delta_J \times \oint_{C_J} \frac{\bar{R}-\bar{R}_1}{R^3_\beta} \, d\ell \qquad (12)$$

where C_J is a line in τ_J parallel to the average direction of $\bar{\gamma}$ in τ_J, δ_J is a distance normal to C_J, and $d\ell$ is the arc length element along C_J. This means that the velocity field induced by a discrete vorticity patch τ_J can be approximated for points outside of τ_J by some mean discrete vortex line whose strength per unit length is $\gamma_J \, \delta_J$. But if the point $\bar{R}_1$ is part of the discrete area τ, the integral in equation (11) has an inherent singularity of the Cauchy type due to the fact that $\bar{R} = \bar{R}_1$ at some point within τ. In order to evaluate the integral expression for this case, consider a point close to $\bar{R}_1$ but located just above τ by a distance ε. As indicated in figure 1, the area of integration in τ is divided into two regions, $A_{\tau-\varepsilon}$ and A_ε. Obviously, the integral over $A_{\tau-\varepsilon}$ has no Cauchy-type singularity, Hadamard's finite part concept being sufficient to perform the indicated integration. Thus,

$$\int_{\tau} \bar{\gamma} \times \frac{\bar{R}-\bar{R}_1}{R_\beta^3}\, dS = \lim_{\epsilon \to o} \int_{A_\epsilon} + \lim_{\epsilon \to o} \int_{A_{\tau-\epsilon}}$$

$$= \lim_{\epsilon \to o} I(\epsilon) + \bar{\gamma}\, \delta \times \int_{C} \frac{\bar{R}-\bar{R}_1}{R_\beta^3}\, d\ell \qquad (13)$$

The last integral in equation (13) represents the conventional discrete vortex line contribution whose evaluation presents no difficulty. In order to determine the integration denoted by $I(\epsilon)$ assume that, for simplicity, the coordinate system is centered at the point $\bar{R}_1$, and that the x-y plane is determined by the discrete area τ. Then, if γ denotes the modulus of $\bar{\gamma}$,

$$I(\epsilon) = \gamma \int_{A_\epsilon} \frac{y \sin\Lambda - x \cos\Lambda}{\{x^2 - B^2 (y^2 + \epsilon^2)\}^{3/2}}\, dx\, dy \qquad (14)$$

where Λ is the angle between the y-axis and the direction of the vorticity in τ, and $B^2 = -\beta^2 > 0$ (supersonic flow). The components of the vector cross product $\bar{\gamma} \times (\bar{R}-\bar{R}_1) = \bar{\gamma} \times \bar{R}$ which are not normal to the plane of τ have been left out of equation (14) because, when the limit operation $\epsilon \to o$ is carried out, they will vanish. The area A_ϵ is bounded by a line parallel to the vorticity direction going through $x = -(1+B)\epsilon$ and by the intersection of the Mach forecone from the point (o, o, ϵ) with the τ-plane, consequently, if the integration with respect to x is performed first,

$$I(\epsilon) = \gamma \cos\Lambda \int_{\lambda_1}^{\lambda_2} \left\{ \int_{ty-(1+B)\epsilon}^{-B\sqrt{y^2+\epsilon^2}} \frac{ty - x}{\{x^2 - B^2 (y^2 + \epsilon^2)\}^{3/2}}\, dx \right\} dy \qquad (15)$$

where $t = \tan\Lambda$, and λ_1, λ_2 are the values of y corresponding to the intersection of the line $x = ty - (1+B)\epsilon$ with the hyperbola $x = -B\sqrt{y^2 + \epsilon^2}$. Let $\phi = \epsilon^2(1+2B) - 2(1+B)\epsilon ty - (B^2 - t^2) y^2$, then the finite part of the x-integration yields

$$I(\epsilon) = \gamma \cos\Lambda \int_{\lambda_1}^{\lambda_2} \left\{ \frac{ty\,(ty-(1+B)\epsilon)}{B^2 (y^2 + \epsilon^2)\sqrt{\phi}} - \frac{1}{\sqrt{\phi}} \right\} dy$$

$$= \frac{\gamma \cos\Lambda}{B^2} \int_{\lambda_1}^{\lambda_2} \left\{ \frac{B^2\epsilon-(1+B)\ \epsilon t y-(B^2-t^2)y^2}{y^2+\epsilon^2} \right\} \frac{dy}{\sqrt{\phi}} \qquad (16)$$

Since ϵ is a very small quantity, the variation of y in the interval (λ_1, λ_2) is going to be equally small, and, therefore, the quantity within brackets in the last integrand of equation (16) can be replaced by a mean value and taken outside of the integral sign. The same is not true of the term $1/\sqrt{\phi}$ since it will vary from ∞ for $y = \lambda_1$, go through finite values in the integration interval, and then again increase to ∞ for $y = \lambda_2$. With this in mind, and if $\tilde{y}$ denotes a mean value of y, $I(\epsilon)$ can be written as

$$I(\epsilon) = \frac{\gamma \cos\Lambda}{B^2} \frac{B^2\epsilon-(1+B)\ \epsilon t\tilde{y} - (B^2-t^2)\ \tilde{y}^2}{\tilde{y}^2+\epsilon^2} \int_{\lambda_1}^{\lambda_2} \frac{dy}{\sqrt{\phi}} \qquad (17)$$

But λ_1, λ_2 are the roots of $ty-\epsilon = -B\sqrt{y^2+\epsilon^2}$, i.e., they are the roots of the polynomial denoted by ϕ. Thus

$$\sqrt{\phi} = \sqrt{\epsilon^2(1+2B)-2(1+B)\epsilon t y\ -(B^2-t^2)\ y^2} = \sqrt{B^2-t^2}\ .\ \sqrt{(\lambda_1-y)(y-\lambda_2)} \qquad (18)$$

Introducing this expression for $\sqrt{\phi}$ into (17), and taking the limit $\epsilon \to o$, the following value for $I(\epsilon)$ is obtained:

$$I(o) = \lim_{\epsilon \to o} I(\epsilon) = -\frac{\gamma \cos\Lambda}{B^2} \sqrt{B^2-t^2} \int_{\lambda_1}^{\lambda_2} \frac{dy}{\sqrt{(\lambda_1-y)(y-\lambda_2)}} \qquad (19)$$

The integral appearing in equation (19) can be easily evaluated by complex variable methods; its value is found to be

$$\int_{\lambda_1}^{\lambda_2} \frac{dy}{\sqrt{(\lambda_1-y)(y-\lambda_2)}} = \pi \qquad (20)$$

The contribution of the inherent singularity to the velocity field, within τ, induced by the vorticity patch τ, and dented herein by w*, is therefore given by

$$w^* = -\frac{\beta^2}{2\pi} \lim_{\varepsilon \to o} I(\varepsilon) = -\frac{\gamma \cos\Lambda}{2} \sqrt{B^2 - t^2} \qquad (21)$$

This contribution is perpendicular to the plane of τ, and it has only physical meaning when $B^2 > t^2$, i.e., when the vortex lines are swept in front of the Mach lines. It is expression (21), taken in conjunction with equations (11) and (12), that makes the vortex lattice method applicable to supersonic flow.

The Skewed-Horseshoe Vortex

Velocity fields due to complex vortex curves can be generated by the linear superposition of fields induced by simple vortex geometries. For instance, the velocity field due to a horseshoe line vortex can be obtained by the addition of the corresponding fields induced by three rectilinear segments: a transverse skewed segment, and two trailing legs, figure 2. Therefore, the determination of the velocity field due to a line vortex segment of constant, but arbitrary, sweep is the fundamental building block in the formulation of aerodynamic influence coefficients of complex three-dimensional vortex lattices. Choosing a coordinate system such that the vortex line lies in the plane z = 0, the conventional discrete vortex contribution to the velocity at a point whose coordinates are (x_o, y_o, z_o) is given, in Cartesian components, by the following expressions

$$u = +\frac{\Gamma z_o}{2\pi K} \beta^2 \oint_C \frac{dy}{\left\{ (x-x_o)^2 + \beta^2 \left((y-y_o)^2 + z_o^2 \right) \right\}^{3/2}}$$

$$v = -\frac{\Gamma z_o}{2\pi K} \beta^2 \oint_C \frac{dx}{\left\{ (x-x_o)^2 + \beta^2 \left((y-y_o)^2 + z_o^2 \right) \right\}^{3/2}} \qquad (22)$$

$$w = +\frac{\Gamma}{2\pi K} \beta^2 \oint_C \frac{(x-x_o)\,dy - (y-y_o)\,dx}{\left\{ (x-x_o)^2 + \beta^2 \left((y-y_o)^2 + z_o^2 \right) \right\}^{3/2}}$$

where Γ represents the circulation per unit length of discrete vortex line length, and the integrations are to be carried out along that part of C which satisfies the conditions

$$(x - x_o)^2 + \beta^2 ((y - y_o)^2 + z_o^2) > 0$$

and

$$x - x_o < 0 \quad \text{if} \quad M_\infty > 1.$$

For the transverse leg of the horseshoe vortex, the coordinate x appearing in equations (22) can be expressed as a function of y, i.e., $x = ty$, and the indicated integrations carried out between the limits $y = -s$ and $y = +s$, figure 2. By defining the following auxiliary variables

$$x_1 = x_o + ts \qquad x_2 = x_o - ts$$

$$y_1 = y_o + s \qquad y_2 = y_o - s$$

$$X^* = x_o - ty_o$$

The resulting formulas giving the velocity components induced by the skewed transverse rectilinear vortex filament can be written as follows:

$$u = + \frac{\Gamma z}{2\pi K} \cdot \frac{1}{x^{*2} + (t^2+\beta^2) z_o^2} \cdot \left[\frac{tx_1 + \beta^2 y_1}{\sqrt{x_1^2 + \beta^2 (y_1^2+z_o^2)}} - \frac{tx_2 + \beta^2 y_2}{\sqrt{x_2^2 + \beta^2 (y_2^2+z_o^2)}} \right]$$

$$v = - \frac{\Gamma z}{2\pi K} \cdot \frac{t}{x^{*2} + (t^2+\beta^2) z_o^2} \cdot \left[\frac{tx_1 + \beta^2 y_1}{\sqrt{x_1^2 + \beta^2 (y_1^2+z_o^2)}} - \frac{tx_2 + \beta^2 y_2}{\sqrt{x_2^2 + \beta^2 (y_2^2+z_o^2)}} \right] \quad (23)$$

$$w = - \frac{\Gamma}{2\pi K} \frac{x^*}{x^{*2} + (t^2+\beta^2) z_o^2} \left[\frac{tx_1 + \beta^2 y_1}{\sqrt{x_1^2 + \beta^2 (y_1^2+z_o^2)}} - \frac{tx_2 + \beta^2 y_2}{\sqrt{x_2^2 + \beta^2 (y_2^2+z_o^2)}} \right]$$

In the above expressions, the coordinates (x_o, y_o, z_o) of the receiving field point are measured with respect to the midpoint of the rectilinear vortex segment, the x-y plane of the coordinate system coinciding with the plane defined by the x-axis and the vortex itself.

The case of a rectilinear vortex segment parallel to the x-axis ($t = \infty$) is of special importance since the trailing legs of a horseshoe vortex are generally assumed to be parallel to the x-axis. Since $dy = 0$, equations (22) become

$$u = 0$$

$$v = -\frac{\Gamma z_o}{2\pi K} \beta^2 \oint_c \frac{dx}{\left\{(x-x_o)^2 + \beta^2 \left((y-y_o)^2 + z_o^2\right)\right\}^{3/2}} \tag{24}$$

$$w = -\frac{\Gamma(y-y_o)}{2\pi K} \beta^2 \oint_c \frac{dx}{\left\{(x-x_o)^2 + \beta^2 \left((y-y_o)^2 + z_o^2\right)\right\}^{3/2}}$$

If the vortex segment extends from $x = x_i$ to $x = x_f$, the above integration yields

$$u = 0$$

$$v = -\frac{\Gamma z_o}{2\pi K}\left[\frac{x_o - x_i}{\sqrt{(x_o-x_i)^2 + \beta^2\left((y_o-y)^2 + z_o^2\right)}} - \frac{x_o - x_f}{\sqrt{(x_o-x_f)^2 + \beta^2\left((y_o-y) + z_o^2\right)}}\right] \frac{1}{(y_o-y)^2 + z_o^2} \tag{25}$$

$$w = +\frac{\Gamma}{2\pi K}\left[\frac{x_o - x_i}{\sqrt{(x_o-x_i)^2 + \beta^2\left((y_o-y)^2 + z_o^2\right)}} - \frac{x_o - x_f}{\sqrt{(x_o-x_f)^2 + \beta^2\left((y_o-y) + z_o^2\right)}}\right] \frac{y_o - y}{(y_o-y)^2 + z_o^2}$$

For a conventional horseshoe vortex whose trailing legs stretch to downstream infinity, equations (25) would give the contribution of the port leg with the following substitutions

$$x_i = \infty \quad \text{if} \quad M_\infty < 1$$

$$x_i = x_o - \sqrt{-\beta^2\left((y_o+s)^2 + z_o^2\right)} \quad \text{if} \quad M_\infty > 1$$

$$x_f = -ts$$

$$y = -s$$

Likewise, the contribution from the starboard trailing leg can be computed by introducing the following values into equations (25)

$$x_i = +ts$$

$$x_f = \infty \quad \text{if} \quad M_\infty < 1$$

$$x_f = x_o - \sqrt{-\beta^2 \left((y_o - s)^2 + z_o^2\right)} \quad \text{if} \quad M_\infty > 1$$

$$y = +s$$

Combining these results with equations (23), the formulas defining the flow field induced by a discrete vortex consisting of a skewed segment and two trailing legs parallel to the x-axis (the skewed-horseshoe vortex) are obtained. Keeping in mind Hadamard's finite part concept, and after introducing the following notation

$$F_1 = \frac{tx_1 + \beta^2 y_1}{\sqrt{x_1^2 + \beta^2 (y_1^2 + z_o^2)}} \quad ;$$

$$F_2 = \frac{tx_2 + \beta^2 y_2}{\sqrt{x_2^2 + \beta^2 (y_2^2 + z_o^2)}} \quad ; \tag{26}$$

$$G_1 = \frac{x_1}{\sqrt{x_1^2 + \beta^2 (y_1^2 + z_o^2)}} + C \quad ; \quad (M_\infty < 1: C = 1; M_\infty > 1: C = 0)$$

$$G_2 = \frac{x_2}{\sqrt{x_2^2 + \beta^2 (y_2^2 + z_o^2)}} + C \quad ; \quad (M_\infty < 1: C = 1; M_\infty > 1: C = 0)$$

then, the horseshoe vortex induced field formulas can be expressed as follows:

$$u(x_o, y_o, z_o) = + \frac{\Gamma}{2\pi K} \frac{z_o}{x^{*2} + (t^2 + \beta^2) z_o^2} (F_1 - F_2)$$

$$v(x_o, y_o, z_o) = + \frac{\Gamma}{2\pi K} z_o \left\{ - \frac{(F_1 - F_2)\, t}{x^{*2} + (t^2 + \beta^2) z_o^2} + \frac{G_1}{y_1^2 + z_o^2} - \frac{G_2}{y_2^2 + z_o^2} \right\} \quad (27$$

$$w(x_o, y_o, z_o) = - \frac{\Gamma}{2\pi K} \left\{ \frac{x^* (F_1 - F_2)}{x^{*2} + (t^2 + \beta^2) z_o^2} + \frac{y_1}{y_1^2 + z_o^2} G_1 - \frac{y_2}{y_2^2 + z_o^2} G_2 \right\}$$

The finite part concept determines the value of the constant C appearing in the definition of G_1 and G_2.

A notable simplification of equations (27) occurs for supersonic flow when the receiving point (x_o, y_o, z_o) is in the plane of the horseshoe, namely, $z_o = 0$. First, the values of the axialwash and sidewash, u and v, vanish identically; secondly, the upwash expression becomes

$$w(x_o, y_o, 0) = - \frac{\Gamma}{2\pi K} \left\{ \frac{F_1 - F_2}{x^*} + \frac{G_1}{y_1} - \frac{G_2}{y_2} \right\} \quad (28$$

Equation (28) is applicable to both subsonic and supersonic flow in its present format. But for the supersonic flow case, the fact that the constant C of the G functions becomes null due to the finite part concept allows further simplification of the upwash equation. Introducing the corresponding values of the F and G functions, the expanded version of equation (28) is

$$w(x_o, y_o, 0) = - \frac{\Gamma}{2\pi K} \left\{ \frac{1}{x^*} \left[\frac{t x_1 + \beta^2 y_1}{\sqrt{x_1^2 + \beta^2 y_1^2}} - \frac{t x_2 + \beta^2 y_2}{\sqrt{x_2^2 + \beta^2 y_2^2}} \right] + \frac{x_1/y_1}{\sqrt{x_1^2 + \beta^2 y_1^2}} - \frac{x_2/y_2}{\sqrt{x_2^2 + \beta^2 y_2^2}} \right\} \quad (29$$

Since $x^* = x_o - ty_o = x_1 - ty_1 = x_2 - ty_2$, the rearrangement of equation (28) in factors of $\left[(x_1 - ty_1)\sqrt{x_1^2 + \beta^2 y_1^2}\right]^{-1}$ and $\left[(x_2 - ty_2)\sqrt{x_2^2 + \beta^2 y_2^2}\right]^{-1}$ finally reduces the upwash formula to

$$w(x_o, y_o\ 0) = -\frac{\Gamma}{2\pi K} \cdot \frac{1}{x^*} \left\{ \frac{\sqrt{x_1^2 + \beta^2 y_1^2}}{y_1} - \frac{\sqrt{x_2^2 + \beta^2 y_2^2}}{y_2} \right\} \tag{30}$$

When the field point $(x_o, y_o, 0)$ is within the distributed vorticity patch which is approximated by the discrete horseshoe vortex, e.g., the control point associated with the horseshoe, the upwash given by equation (30) has to be complemented by the distribution due to the generalized principal part of the upwash integral, as given by equation (21). If δx is the distance, measured in the x-direction, occupied by the distributed vorticity γ which has been lumped into the discrete transverse vortex leg of circulation Γ, the relationship between the γ of equation (21) and the Γ of equations (27) and (30) is

$$\Gamma = \gamma \cos \Lambda\, \delta x \tag{31}$$

Modeling of Lifting Surfaces with Thickness

The method of quadrilateral vortex rings placed on the actual body surface (ref. 1) provides a way of computing the surface pressure distribution of arbitrary bodies using discrete vortex lines only. Numerical difficulties may occur when the above method is applied to the analysis of airfoils with sharp trailing edges due to the close proximity of two vortex surfaces of nearly parallel direction. An alternative approach, requiring somewhat less computer storage and easier to handle numerically, consists in using a double, or biplanar, sheet of swept horseshoe vortices to model a lifting surface with thickness, as shown schematically in figure 3. This constitutes an approximation to the true location of the singularities, similar in nature to the classical lifting surface theory approximation of a cambered sheet.

All the swept horseshoe vortices, and their boundary condition control points, corresponding to a given surface, upper or lower, are located in a same plane. The upper and lower surface lattice planes are separated by a gap which represents the chordwise average of the airfoil thickness distribution. The results are not too sensitive to the magnitude of this gap; any value between one half to the full maximum chordwise thickness of the airfoil has been found to be adequate, the preferred value being two thirds of the maximum thickness. Furthermore, the gap can vary in the direction normal to the x-axis to allow for spanwise thickness taper. On the other hand, the chordwise distribution, or spacing, of the transverse elements of the horseshoe vortices have a significant influence on the accuracy of the computed

surface pressure distribution. For greater accuracy, for a given chordwise number of horseshoe vortices, the transverse legs have to be longitudinally spaced according to the cosine distribution law

$$x_J^v - x_o = \frac{c}{2}\left[1 - \cos\left(\pi \frac{2J-1}{2N}\right)\right] \tag{32}$$

where $x_J^v - x_o$ represents the distance from the leading edge to the midpoint of the swept leg of the Jth horseshoe vortex, c is the length of the local chord running through the midpoints of a given chordwise strip, and N is the number of horseshoe vortices per strip. The chordwise control point location corresponding to this distribution of vortex elements is given by

$$x_J^C - x_o = \frac{c}{2}\left[1 - \cos\left(\pi \frac{J}{N}\right)\right] \tag{33}$$

The control points are located along the centerline, or midpoint line, of the chordwise strip (fig. 4). Lan has shown (ref. 7) that the chordwise 'cosine' collocation of the lattice elements, defined by equations (32) and (33), greatly improve the accuracy of the computation of the effects due to lift. His results are directly extendable to the computation of surface pressure distributions of wings with thickness by the biplanar lattice scheme presented herein.

The small perturbation boundary condition

$$\bar{v} \cdot \bar{n}' = -\bar{u}_\infty \cdot \bar{n} \tag{34}$$

is applied at the control points. In equation (34), $\bar{n} = \ell\bar{I} + m\bar{J} + n\bar{k}$, and $\bar{n}' = m\bar{J} + n\bar{k}$, where ℓ, m, and n are the direction cosines of the normal to the actual airfoil surface. Equation (34) implies that $|\ell u| \ll |mv + nw|$. The use of the small perturbation boundary condition is consistent with the present biplanar approach to the simulation of thick wings.

Modeling of Fusiform Bodies

The modeling of fusiform bodies with horseshoe vortices requires a special concentrical vortex lattice if the simulation of the volume displacement effects, and the computation of the surface pressure distribution, are to be carried out. To define this lattice, it is necessary to consider first an auxiliary body, identical in cross-sectional shape and longitudinal area distribution to the actual body, with a straight baricentric line, i.e., without camber. The cross-sectional shape of this auxiliary body is then approximated by a polygon whose sides determine the transverse legs of the horseshoe vortices. The vertices of the polygon and the axis of the auxiliary body (which by definition is rectilinear (zero camber) and internal to all possible cross sections of the body) define a set of radial planes in which

the bound trailing legs of the horseshoe vortices lie parallel to the axis (fig. 5). As the body cross section changes shape along its length, the corresponding polygon is allowed to change accordingly, but with the constraint that the polygonal vertices must always lie in the same set of radial planes. The axial spacing of the cross-sectional planes that determine the transverse vortex elements, or polygonal rings, follows the cosine law of equation (32). The boundary condition control points are located on the auxiliary body surface, and in the bisector radial planes, with their longitudinal spacing given by equation (33).

The boundary condition to be satisfied at these control points is the zero mass flux equation.

$$\bar{w} \cdot \bar{n} = - \bar{u}_{\infty} \cdot \bar{n} \tag{35}$$

where all the components of the scalar product $\bar{w} \cdot \bar{n} = \beta^2 \ell u + mv + nw$ are to be retained. Thus, equation (35) is a higher order condition than equation (34). The use of this higher order boundary condition, within the framework of a linearized theory, is not mathematically consistent. Therefore, it can only be justified by its results rather than by a strict mathematical derivation. In the present treatment of fusiform bodies, it has been found that the use of higher order, or exact boundary conditions is a requisite for the accurate determination of the surface pressure distribution.

The fact that the vector $\bar{w}$, instead of $\bar{v}$, appears in the left hand member of equation (35) requires some elaboration. First, it should be pointed out that for small perturbations $\bar{w} \cdot \bar{n} \cong \bar{v} \cdot \bar{n}'$. Furthermore, for incompressible flow ($\beta = 1$), the vector $\bar{w}$ is identical to the perturbation velocity $\bar{v}$. Consequently, the boundary condition equation (34) is consistent with the continuity equation, $\nabla \cdot \bar{w} = 0$, to a first order for compressible flow, and to any higher order for incompressible flow. But when a higher order boundary condition is applied in compressible flow to a linearized solution, it should be remembered that this solution satisfies the conservation of $\bar{w}$, not of $\bar{v}$, i.e., $\nabla \cdot \bar{w} = 0$. Thus, the higher order boundary condition should involve the reduced current velocity, or perturbation mass flux, vector $\bar{w}$, as in equation (35), rather than the perturbation velocity vector $\bar{v}$.

The body camber, which was eliminated in the definition of the auxiliary body, is taken into account in the computation of the direction cosines ℓ, m, and n, which are implicit in equation (35). Therefore, the effect of camber is represented in the boundary condition but ignored in the spatial placement of the horseshoe elements. This scheme will give a fair approximation to cambered fusiform bodies provided that the amount of body camber is not too large.

Computation of Sideslip Effects

The aerodynamics of an isolated wing in sideslip can be analyzed by two different approaches depending on the coordinate system chosen. In one approach, the coordinate system consists of wind axes, the longitudinal axis being aligned with the free-stream velocity vector, figure 6. This formulation of the problem is known as the skewed-wing approach, and a first order solution obtained within this framework will give the dominant effects of sideslip, even for the case of zero dihedral. The other approach, also shown schematically in figure 6 and known as the skewed free-stream approach, is based on a body-axis formulation of the problem and the corresponding first order solution, though it may be adequate for large dihedral, will fail to produce the significant effects of sideslip for low or zero dihedral. To compute the sideslip effects correctly within the framework of a skewed free-stream formulation, it is necessary to solve partial differential equations containing second order terms of the perturbation velocities. This implies a much more involved computational procedure than that required for the solution of the first order perturbation equations (1) On the other hand, the application of the skewed-wing approach to anything more complex than an isolated wing in sideslip, such as might be the case with a configuration with wing, fuselage, and nacelles, becomes geometrically very complicated.

The approach adopted herein is a combination of the two approaches mentioned above, formulated with the objective of obtaining reasonably accurate sideslip effects using only a first order perturbation solution but without all of the geometrical complications inherent in the skewed-wing approach. Basically it is assumed that the vortex lattice representing the configuration and its vortex wake consists of both bound and free elements or legs; the vortex filaments that model rigid surfaces are considered bound, and those that constitute the wake are the so-called free elements, figure 7. The bound portion of the lattice, containing both transverse and trailing, or chordwise, segments, is invariant in a body axis system, the chordwise legs being parallel to the x-axis. The free legs of the lattice are not actually force free, rather they are assumed to extend to downstream infinity parallel to a predetermined direction which is proportional to the angles of attack and sideslip. If the proportionality factors are unity, then the free portion of the lattice would be invariant in wind axes.

After the circulation strengths of the above lattice geometry are solved for under the appropriate boundary conditions, the pressure coefficient distribution is computed in accordance with the higher order expression

$$c_p = -\frac{2}{q_\infty^2}\,(U_\infty u + V_\infty v) \tag{36}$$

where U_∞ and V_∞ are the components along the x and y body axes of the free-stream velocity vector of modulus q_∞; the corresponding perturbation velocity components are denoted by u and v, as usual. The use of equation (36) instead of the linear approximation

$$C_p = -\frac{2}{q_\infty^2} U_\infty u \qquad (37)$$

is required for the correct computation, within the present framework, of the rolling moment due to sideslip of a planar wing. This is due to the fact that the bound trailing legs, being defined in body axes, are not lined up with the free-stream flow and therefore, according to the theorem of Kutta, they contribute to the normal force. This contribution is represented by the second order term in equation (36), namely, $V_\infty v$. Even though this contribution is of second order, it must be included in the computation of the differential rolling moment due to sideslip, since this quantity itself is of the second order for a planar, or nearly planar, wing.

THE GENERALIZED VORTEX LATTICE METHOD

Description of Computational Method

The four items discussed in the preceding section, i.e., the inclusion of the vorticity-induced residual term w* for supersonic flow, the biplanar scheme for representing thickness effects, the use of a vortex grid of concentrical polygonal cylinders for the simulation of fusiform bodies, and the special lattice geometry consisting of both bound and free elements for the analysis of sideslip effects, have been implemented in a computational procedure herein known as the generalized vortex lattice (GVL) method. This method, outlined in what follows, has been codified in a Fortran IV computer program (VORLAX).

The basic element of the method is the swept horseshoe vortex whose trailing legs has both bound and free segments. The latter segments may trail to downstream infinity in any arbitrary, but predetermined, direction whereas the bound trailing legs are laid out on the proper cylindrical control surfaces in a direction which is parallel to the x body axis. Figure 8 illustrates schematically the representation of a wing-body configuration within the context of the present method. In this illustration, the streamwise arrangement of the lattice follows the cosine distribution law, equation (32), but both chordwise and spanwise distributions of vortex lines can be independently specified to be either of the cosine or of the equal spacing. To each horseshoe vortex there corresponds a control point which is placed midway between the bound trailing legs of the horseshoe; the longitudinal location of the control point is determined by equation (33) if the cosine chordwise distribution has been chosen, otherwise it is located halfway between the transverse legs, as required by quarter-chord/three-quarter-chord rule.

The direction of floatation of the wake vortex filaments is defined by the two angles α_ν and β_ν shown in figure 8, the former being proportional to the angle of attack, and the latter being proportional to the sideslip angle. The proportionality constants are part of the program input, the recommended values being 0 for the sideslip constant, and 0 or 0.5 for the angle of attack constant.

The velocity field induced by the elementary horseshoe vortex is given by equations (27) when above constants are both zero, and by somewhat more complicated expressions which take into account the kinks in the trailing legs when either one or both of the wake floatation parameters are nonzero. Though not presented here, these expressions can be easily derived through the application of equations (23).

When the influence induced by a horseshoe vortex upon its own control point is being evaluated, the contribution from the generalized principal part, as given by equation (21), is included in the normalwash if the free-stream is supersonic. Furthermore, for the supersonic case, the simplified downwash formula, equation (30), is used whenever the receiving point is in the same plane of the inducing horseshoe.

The horseshoe vortex velocity field is used to generate the coefficients of a system of linear equations relating the unknown vortex strengths to the appropriate boundary condition at the control points. This linear system is solved by either a Gauss-Seidel iterative procedure, known as controlled successive over-relaxation (ref. 8), or by a vector orthogonalization technique, i.e., Purcell's vector method (ref. 9). If the inverse process is desired, i.e., synthesis or design instead of analysis, the linear system of equations is used to compute the slope distribution (surface warp) required to achieve a specified surface loading; this involves a straightforward matrix multiplication process. Mixed cases, i.e., design and analysis, are easily handled by proper grouping of the boundary condition equations.

The pressure coefficients are computed in terms of the perturbation velocity components, the computation being carried out according to either one of three possible ways, as follows:

1. If the surface under consideration is assumed wetted by the flow on both sides (zero thickness panel) and the configuration sideslip angle is zero, then a net loading coefficient is computed based on the local value of the spanwise vorticity, namely, $\Delta Cp = 2\gamma \cos\Lambda$;

2. When the configuration sideslip angle is not zero, the net loading coefficient of a zero-thickness surface is calculated through the use of the higher order expression (36); and

3. When surface pressure coefficients are computed, i.e., the panel under consideration is assumed wetted by the flow on one side only, the isentropic flow relationship giving the pressure coefficient in terms of free-stream Mach number and local-to-free-stream velocity ratio is resorted to.

The force and moment coefficients are calculated by numerical integration of the pressure coefficient distribution with due account being given to the edge forces. If cosine chordwise lattice spacing is specified by the VORLAX program user, the computation of the leading edge suction of zero thickness

panels is carried out according to Lan's procedure (ref. 7), whose application to supersonic flow is made possible by the generalized vortex-induced velocity field formulas presented in this report. If equal chordwise lattice spacing is specified, the contribution of the leading edge suction singularity to the forces and moments is calculated by the technique indicated by Hancock in reference 10; this approach is not nearly as accurate as Lan's, the magnitude of the leading edge suction being significantly underestimated.

The VORLAX computer program has the capability of analyzing symmetrical and asymmetrical cases as well as configurations in steady state angular rotation about any or all of three axes, parallel to the coordinate axes, going through the input moment reference center. Steady state angular rotation cases are treated by the subterfuge of assuming a nonuniform onset flow, this onset flow being defined by the values of the angular rates and distance of the field point to the rotation center.

Ground proximity effects are analyzed by the method of images, i.e., the configuration is mirrored about the ground plane; the flow around the airplane and its image then contains a stream surface which coincides with the ground plane due to the symmetry of the arrangement. In this modeling of a configuration in ground proximity, it is assumed that the trailing vorticity wake floats to downstream infinity parallel to the plane of the ground.

Numerical Considerations

At supersonic Mach numbers, the velocity induced by a discrete horseshoe vortex becomes very large in the very close proximity of the envelope of Mach cones generated by the transverse leg of the horseshoe. At the characteristic envelope surface itself, the induced velocity correctly vanishes, due to the finite part concept. This singular behavior of the velocity field occurs only for field points off the plane of the horseshoe. For the planar case, the velocity field is well behaved in the vicinity of the characteristic surface. A simple procedure to treat this numerical singularity consists of defining the characteristic surfaces by the equation

$$(x-x_1)^2 = C\,B^2\left\{(y-y_1)^2 + (z-z_1)^2\right\} \tag{38}$$

where C is a numerical constant whose value is greater than, but close to, 1. It has been found that this procedure yields satisfactory results, and that these results are quite insensitive to reasonable variations of the parameter C.

Another numerical problem, peculiar to the supersonic horseshoe vortex, exists in the planar case (field point in the plane of the horseshoe) when the field point is close to a transverse vortex leg swept exactly parallel to the Mach lines (sonic vortex), while the vortex lines immediately in front of and

behind this sonic vortex are subsonic and supersonic, respectively. This problem can be handled by replacing the boundary condition equation for such sonic vortex with the averaging equation

$$-\gamma_I{}^*_{-1} + 2\,\gamma_I{}^* - \gamma_I{}^*_{+1} = 0 \qquad (39)$$

where $\gamma_I{}^*$ is the circulation strength of the critical horseshoe vortex, and $\gamma_I{}^*_{-1}$ and $\gamma_I{}^*_{+1}$ are the respective circulation values for the fore-and-aft adjacent subsonic and supersonic vortices.

The axialwash induced velocity component (u) is needed for the computation of the surface pressure distribution, and for the formulation of the boundary condition for fusiform bodies. When the field point is not too close to the generating vorticity element, the axialwash is adequately described by the conventional discrete horseshoe vortex representation. But if this point is in the close vicinity of the generating element, as may occur in the biplanar and in the concentrical cylindrical lattices of the present method, the error in the computation of the axialwash due to the discretization of the vorticity becomes unacceptable. This problem is solved by resorting to a vortex-splitting technique, similar to the one presented in reference 11. Briefly, this technique consists of computing the axialwash induced by the transverse leg of a horseshoe as the summation of several transverse legs longitudinally redistributed, according to an interdigitation scheme, over the region that contains the vorticity represented by the single discrete vortex. This is done only if the point at which the axialwash value is required lies within a given near field region surrounding the original discrete vortex.

COMPARISON WITH OTHER THEORIES AND EXPERIMENTAL RESULTS

Conical flow theory provides a body of exact results, within the context of linearized supersonic flow, for some simple three-dimensional configurations. These exact results can be used as bench mark cases to evaluate the accuracy of numerical techniques. This has been done rather extensively for the GVL method, and very good agreement between it and conical flow theory has been observed in the computed aerodynamic load distribution and all force and moment coefficients. Only some typical comparisons are presented in this report, figures 9 through 12.

Finally, the capability of computing surface pressure distributions by the method of this paper is illustrated in figures 13 and 14.

CONCLUDING REMARKS

The present vortex lattice method, in the form of a computer program, has the capability to calculate the aerodynamic load distribution at subsonic and supersonic Mach numbers for arbitrary nonplanar configurations. It has been found to be a very useful preliminary design tool, particularly when aircraft configurations whose mission requirements involve both subsonic and supersonic flight are considered. It is also capable of the inverse process, namely, the computation of the surface warp required to achieve a given load distribution. Correlation with experimental data and with results from other theories shows a good agreement not only in the overall force and moment coefficients due to lift, but also in the distribution of the load coefficients.

The schemes shown for the simulation of thickness and volume effects, which allow the computation of surface pressure distribution by using only vortex lattice singularities, appear adequate for most practical purposes, though experience in this respect is somewhat limited.

The treatment of sideslip cases by the present method does not require higher order solutions, as is necessary for the skewed free-stream approach, and it is not as geometrically complicated as the skewed-wing formulation. Yet the analysis of complex configurations in sideslip still requires care and caution due to the numerical anomalies that may result from the interaction among aircraft components, such as a horizontal tail or a body, and the "free" trailing legs of the horseshoe vortices.

Additional capabilities that can be added to the present computer code, and that would enhance the value of the method as a preliminary design tool include the following:

- Incorporation of an optimization algorithm based either on Lagrange multipliers or on a gradient method, to design the surface warp for minimum drag under specified constraints.

- Application of the technique of reference 11, or of some other adequate technique, for the simulation of jet exhaust effects, with particular attention to its extension to supersonic flow.

- Introduction of a design procedure for the calculation of the geometry required to achieve a given surface pressure distribution, i.e., synthesis of both camber and thickness. The biplanar vortex lattice simulation of a thick lifting surface is well suited for the development of such a design procedure when combined with an iterative scheme.

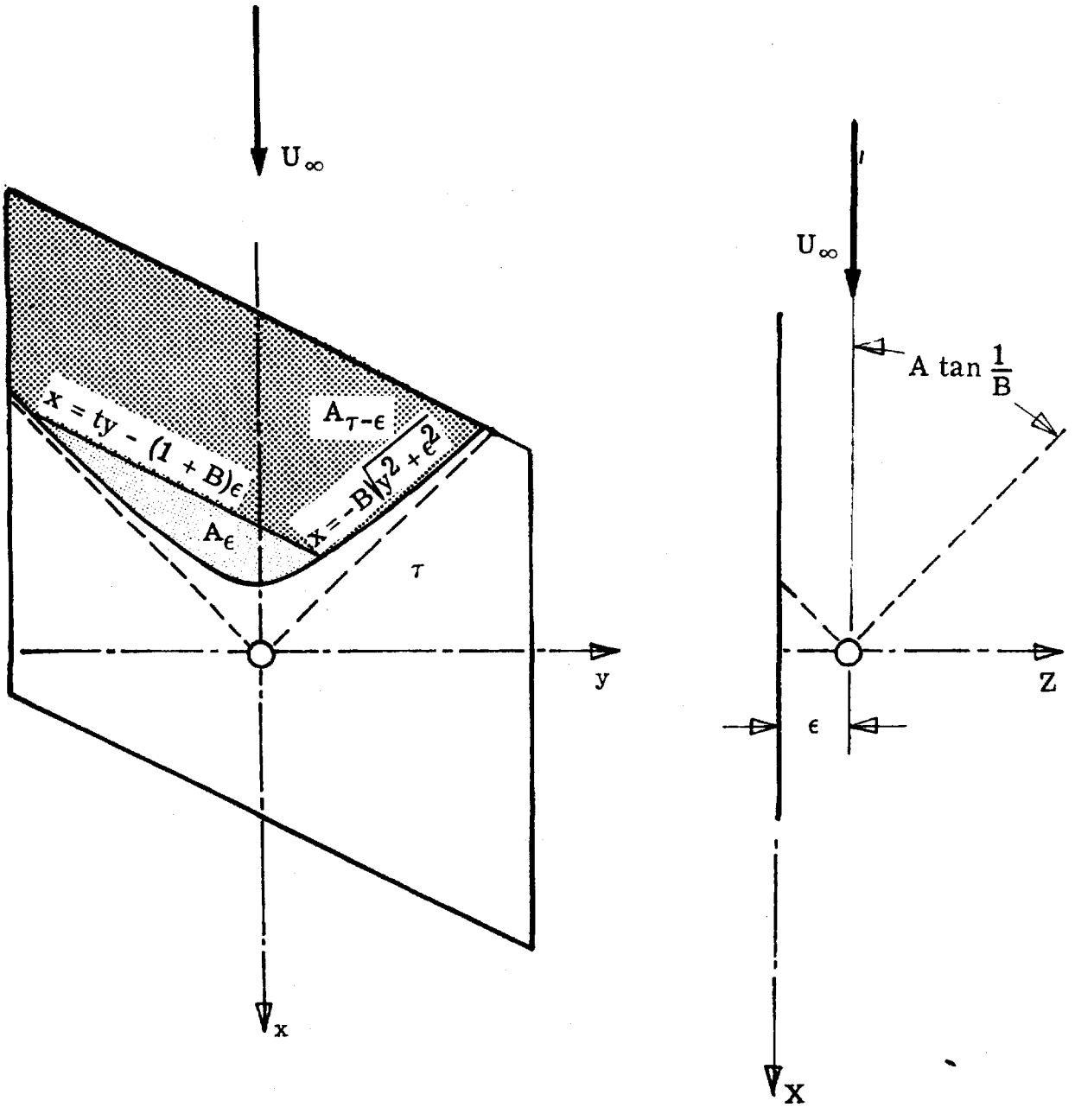

Figure 1.- Definition of integration regions for the computation of principal part.

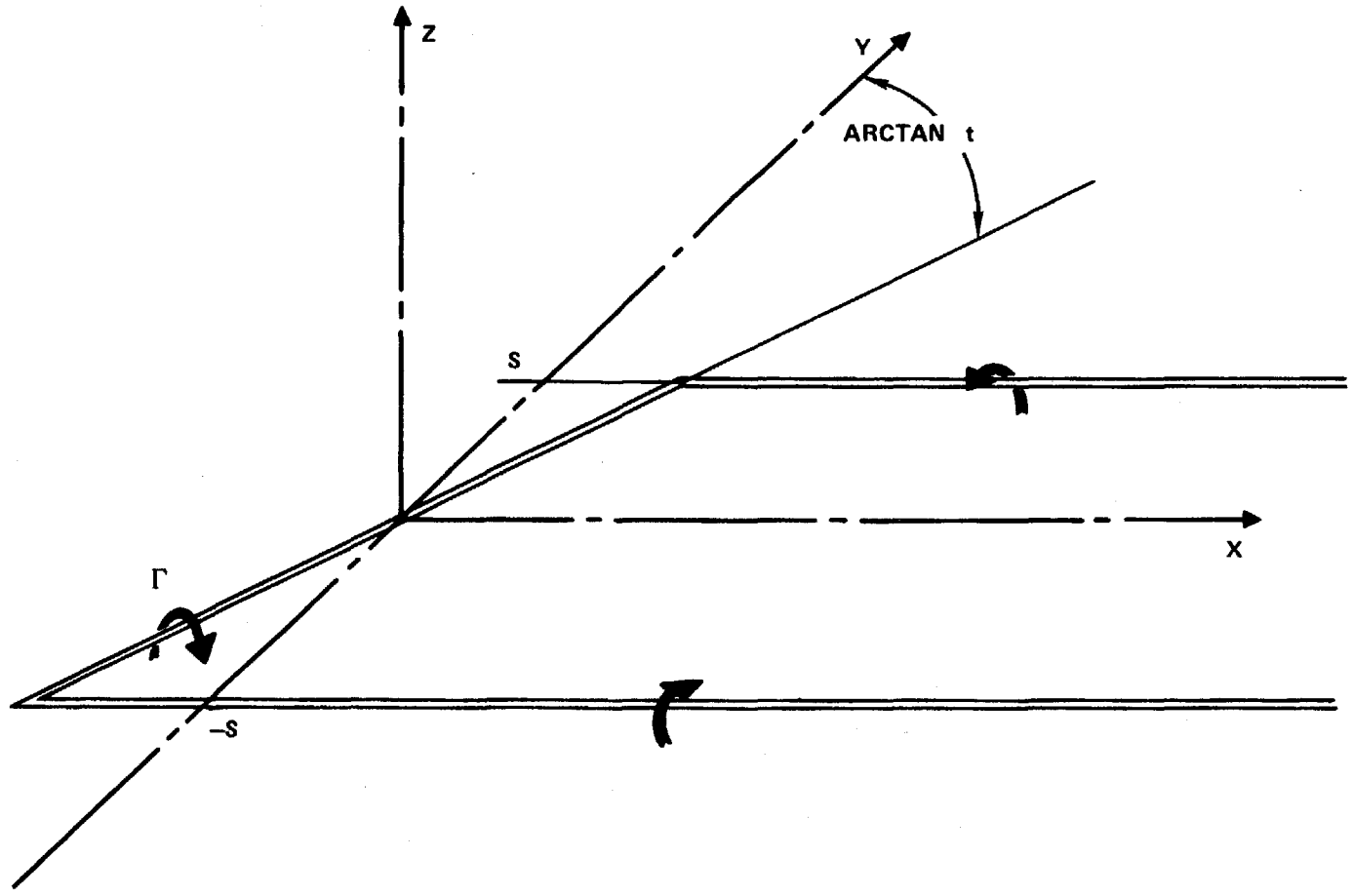

Figure 2.- Sweptback horseshoe vortex

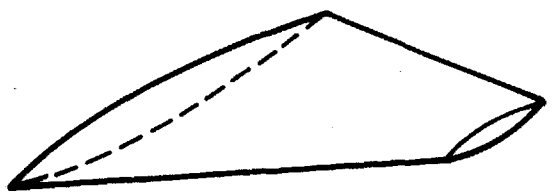

ACTUAL WING PANEL

BOUNDARY CONDITION: $\bar{w} \cdot \bar{n}' = \bar{v} \cdot \bar{n}' = -\bar{u}_\infty \cdot \bar{n}$; $\bar{n}' = m\bar{j} + n\bar{k}$

THIN PANEL LATTICE

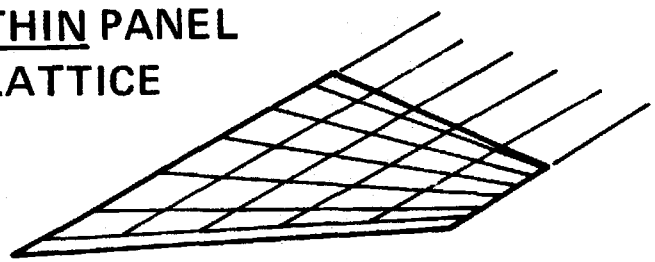

THICK PANEL LATTICE

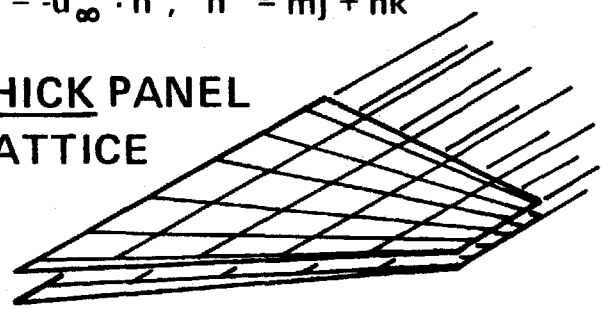

CHORDWISE DISTRIBUTION OF VORTEX LINES: $\frac{X_j^v - X_o}{C} = \frac{1}{2}\left\{1 - \cos\left(\pi \frac{2J-1}{2N}\right)\right\}$

CHORDWISE DISTRIBUTION OF B.C. CONTROL POINTS: $\frac{X_j^c - X_o}{C} = \frac{1}{2}\left\{1 - \cos\left(\pi \frac{J}{N}\right)\right\}$

Figure 3.- Modeling of thick wing with horseshoe vortices.

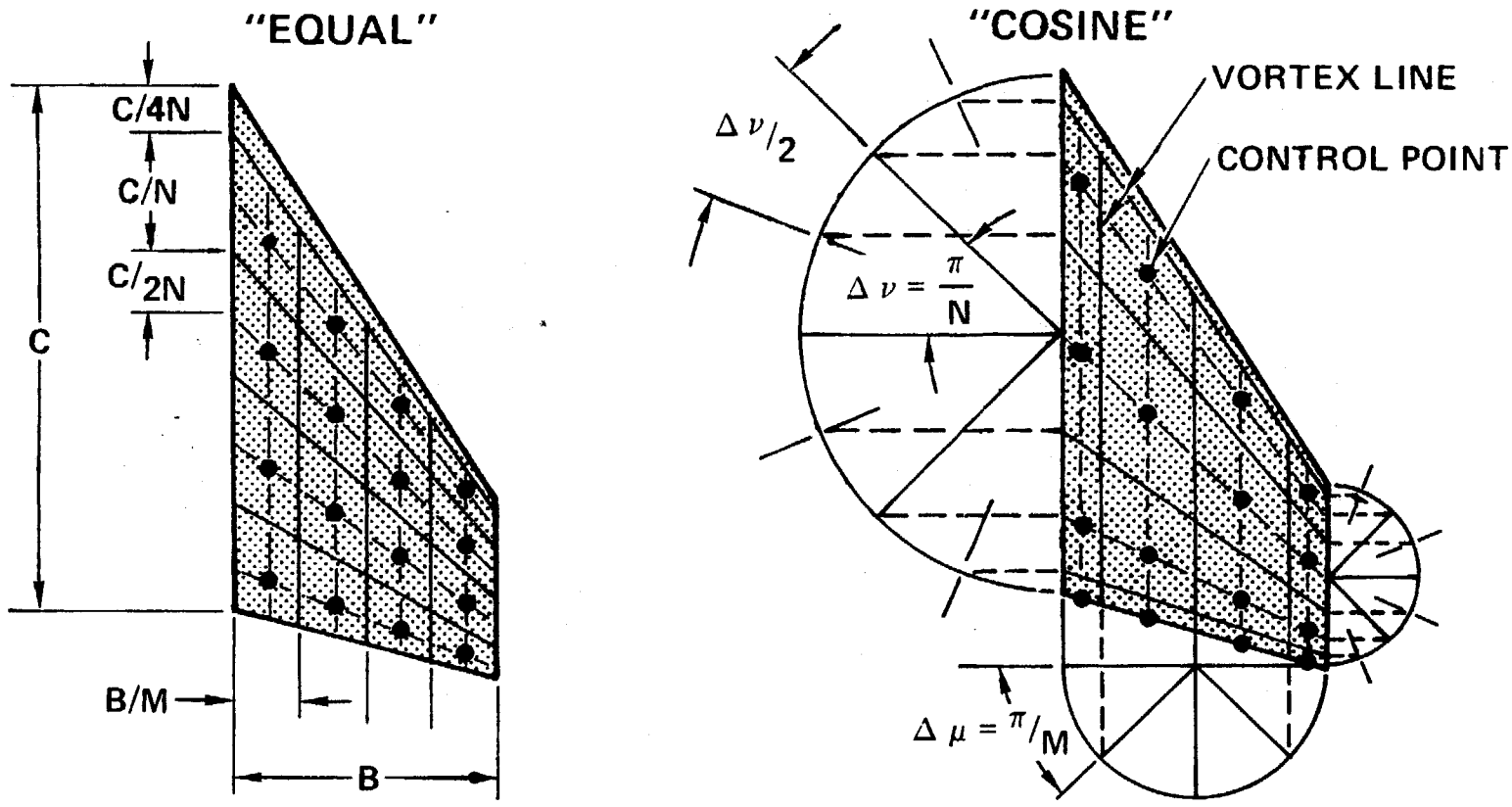

Figure 4.- Vortex lattice collocation.

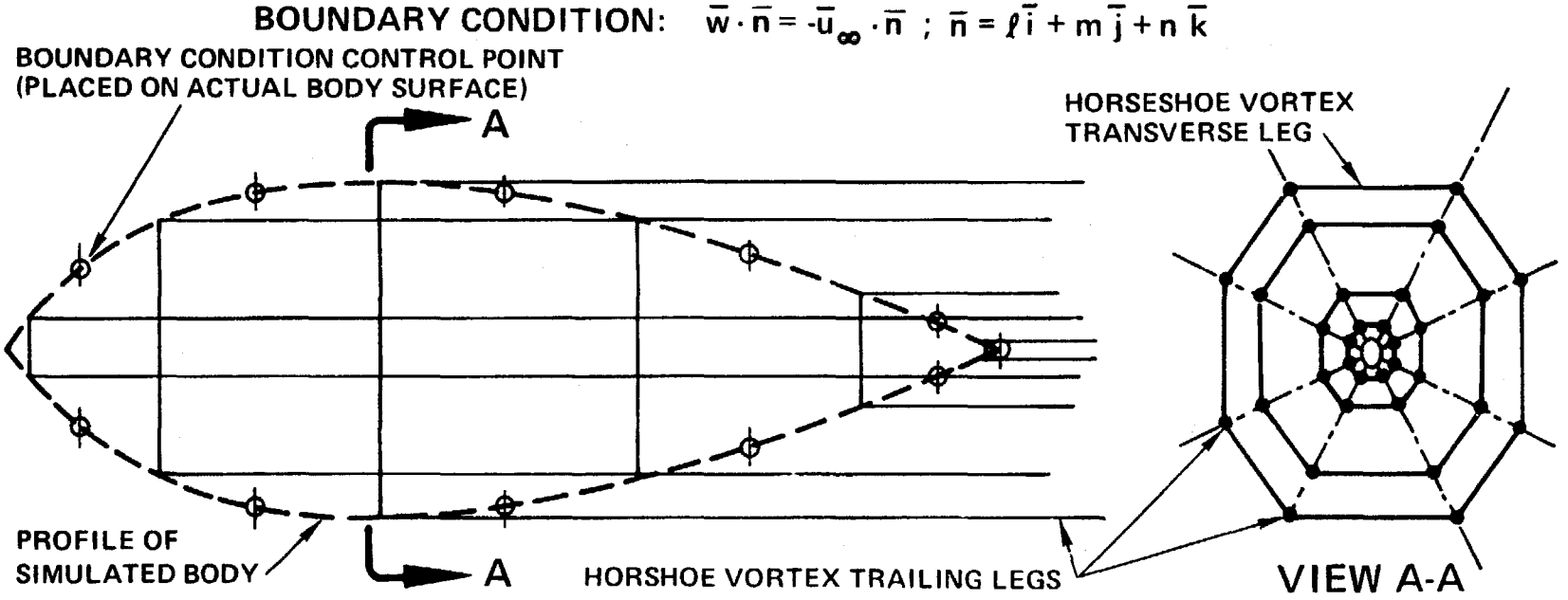

AXIAL DISTRIBUTION OF VORTEX LINES: $\frac{X_j^v - X_o}{L} = \frac{1}{2}\left\{1 - \cos\left(\pi \frac{2J-1}{2N}\right)\right\}$

AXIAL DISTRIBUTION OF B.C. CONTROL POINTS: $\frac{X_j^c - X_o}{L} = \frac{1}{2}\left\{1 - \cos\left(\pi \frac{J}{N}\right)\right\}$

Figure 5.- Modeling of fusiform body with horseshoe vortices.

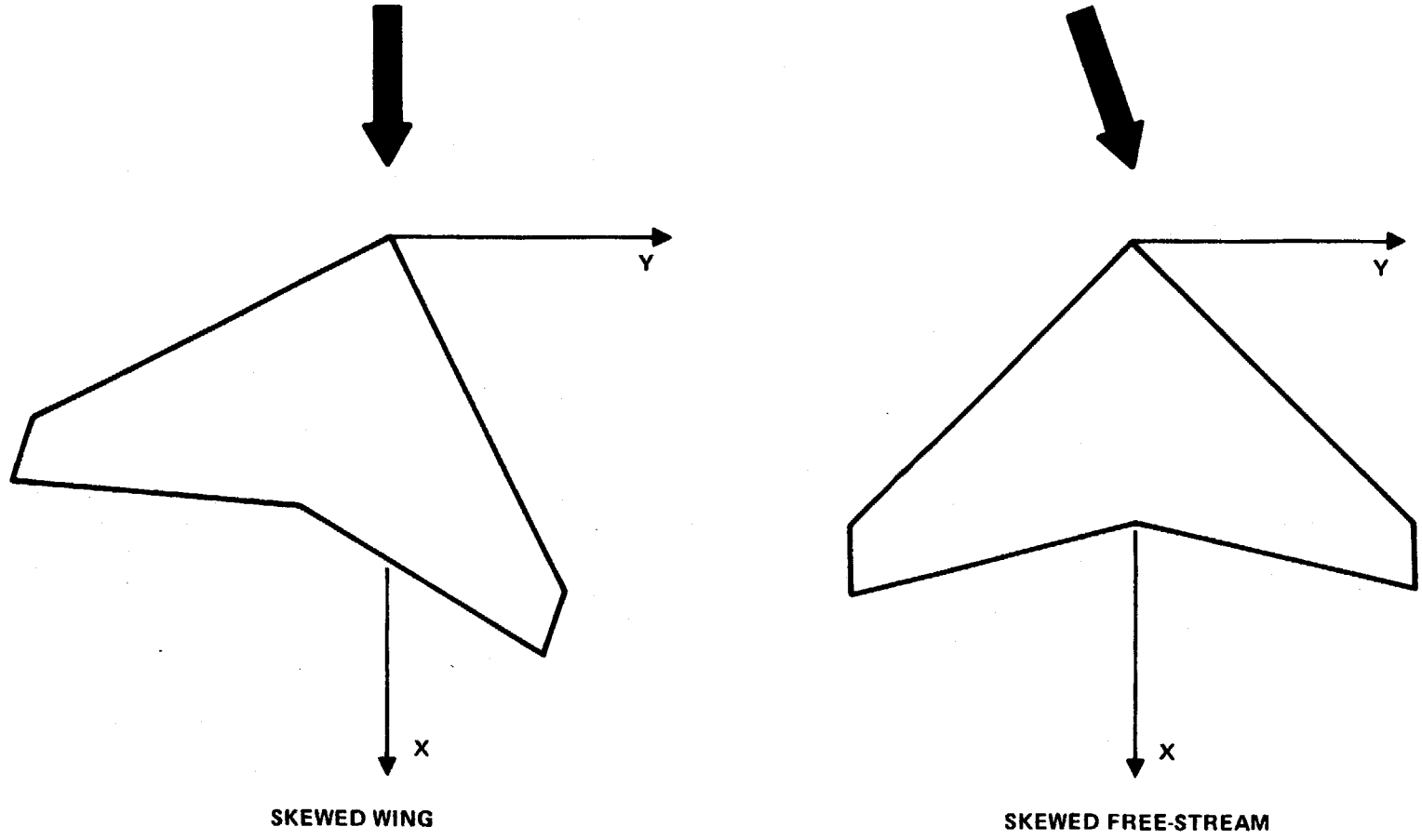

Figure 6.- Conventional approaches for analysis of wing in sideslip.

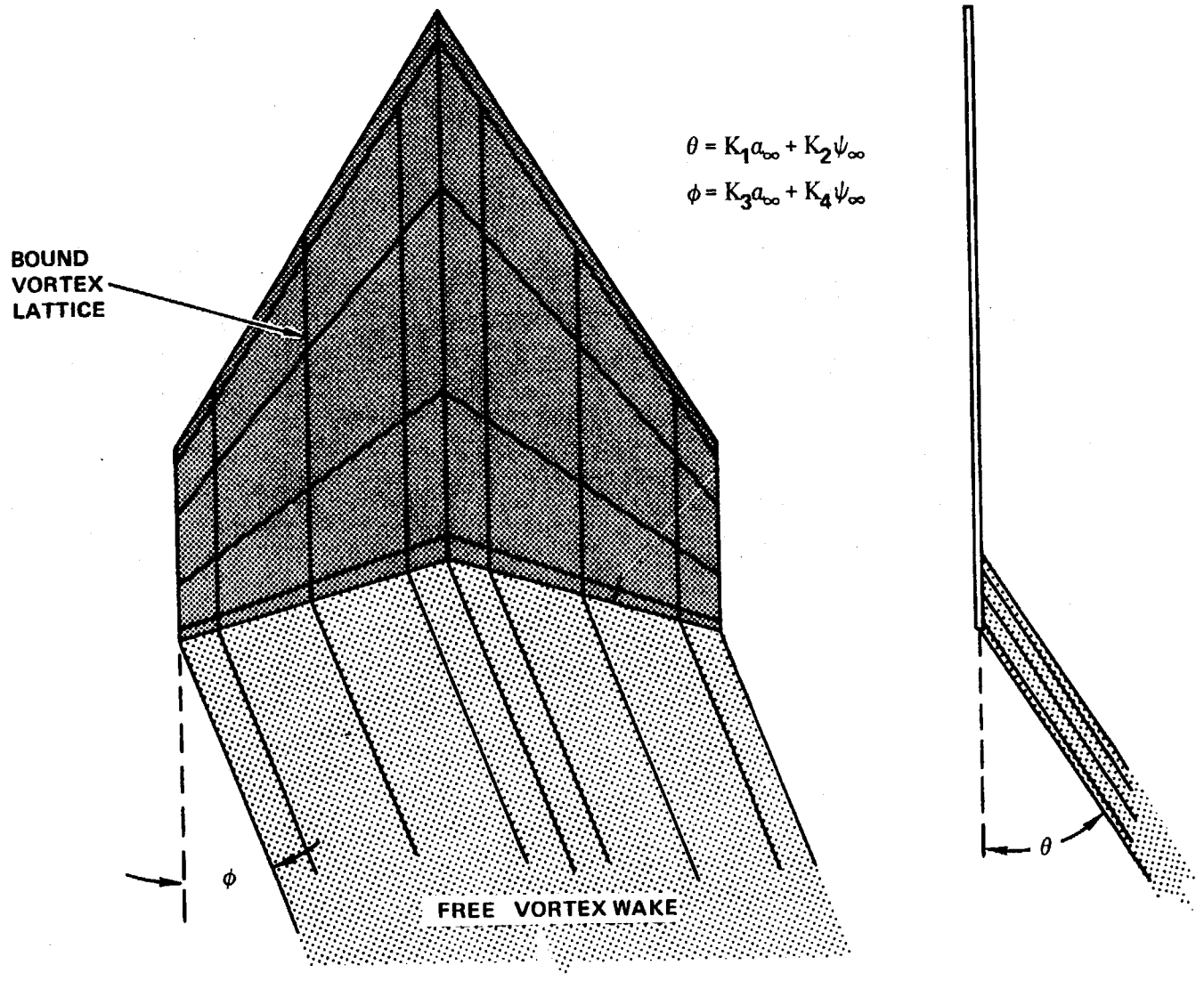

Figure 7.- Lattice geometry for analysis of wing in sideslip.

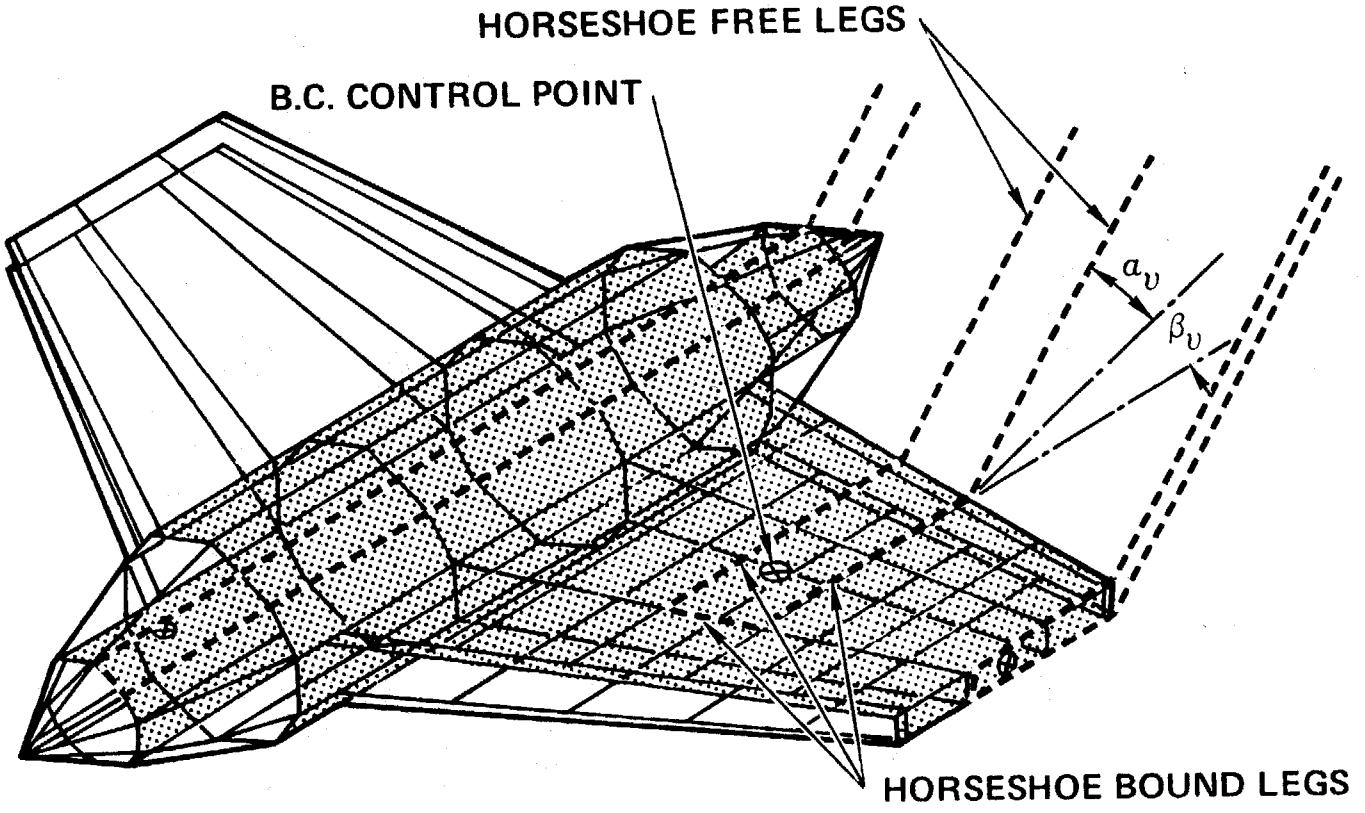

Figure 8.- Generalized vortex lattice model of wing-body configuration.

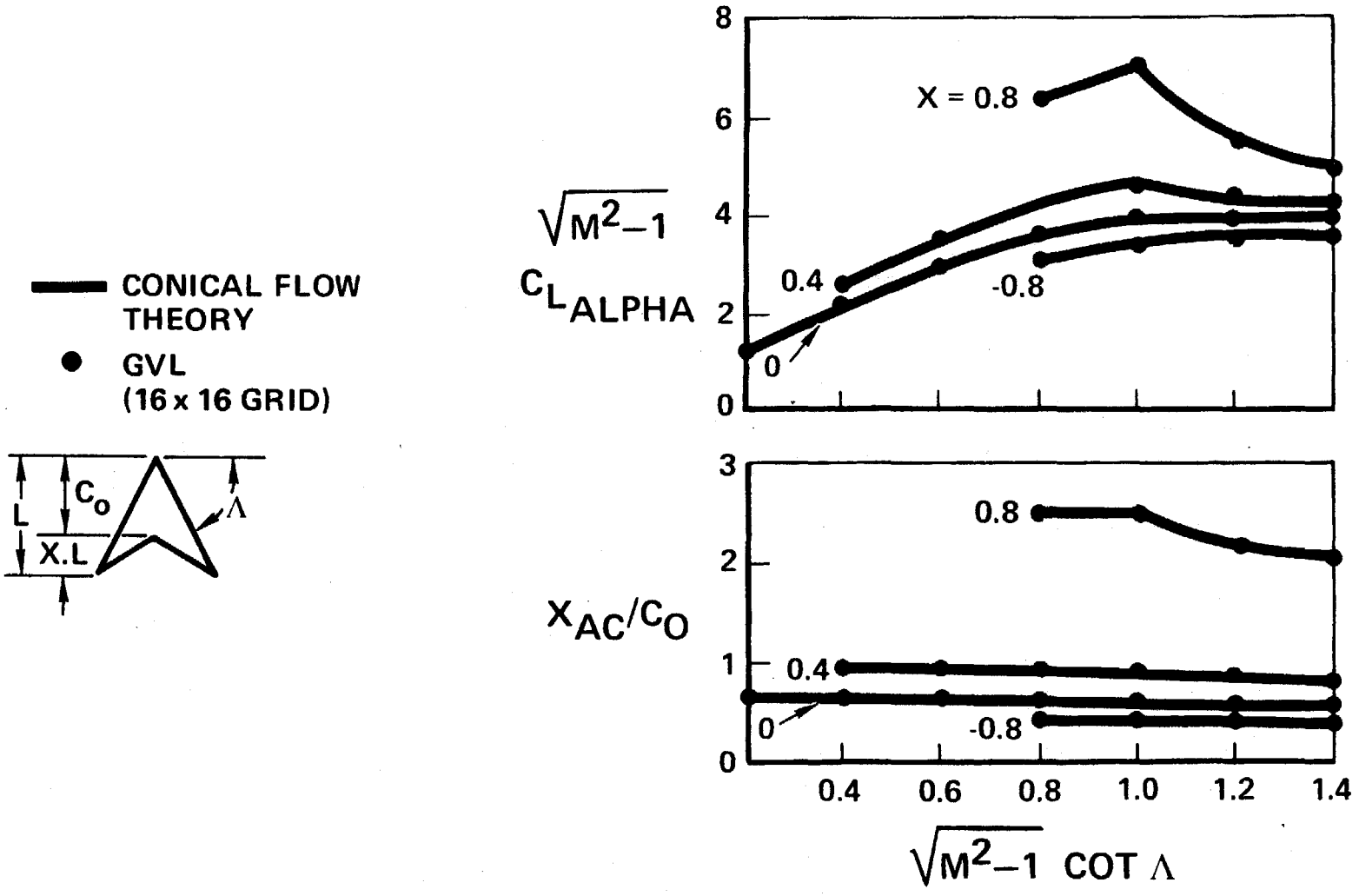

Figure 9.- Theoretical comparison of arrow wing lift slope and aerodynamic center location.

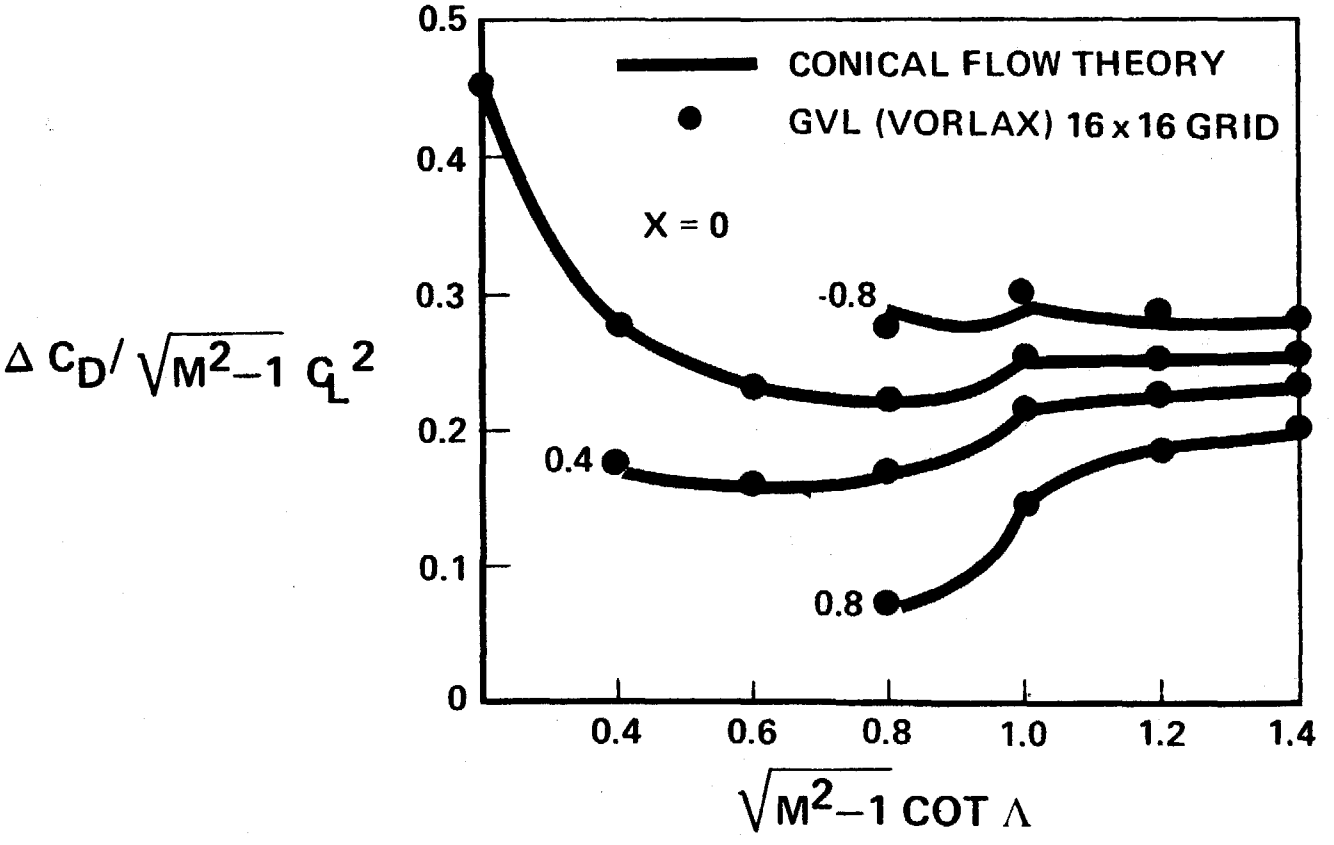

Figure 10.- Theoretical comparison of arrow wing drag-due-to-lift factor.

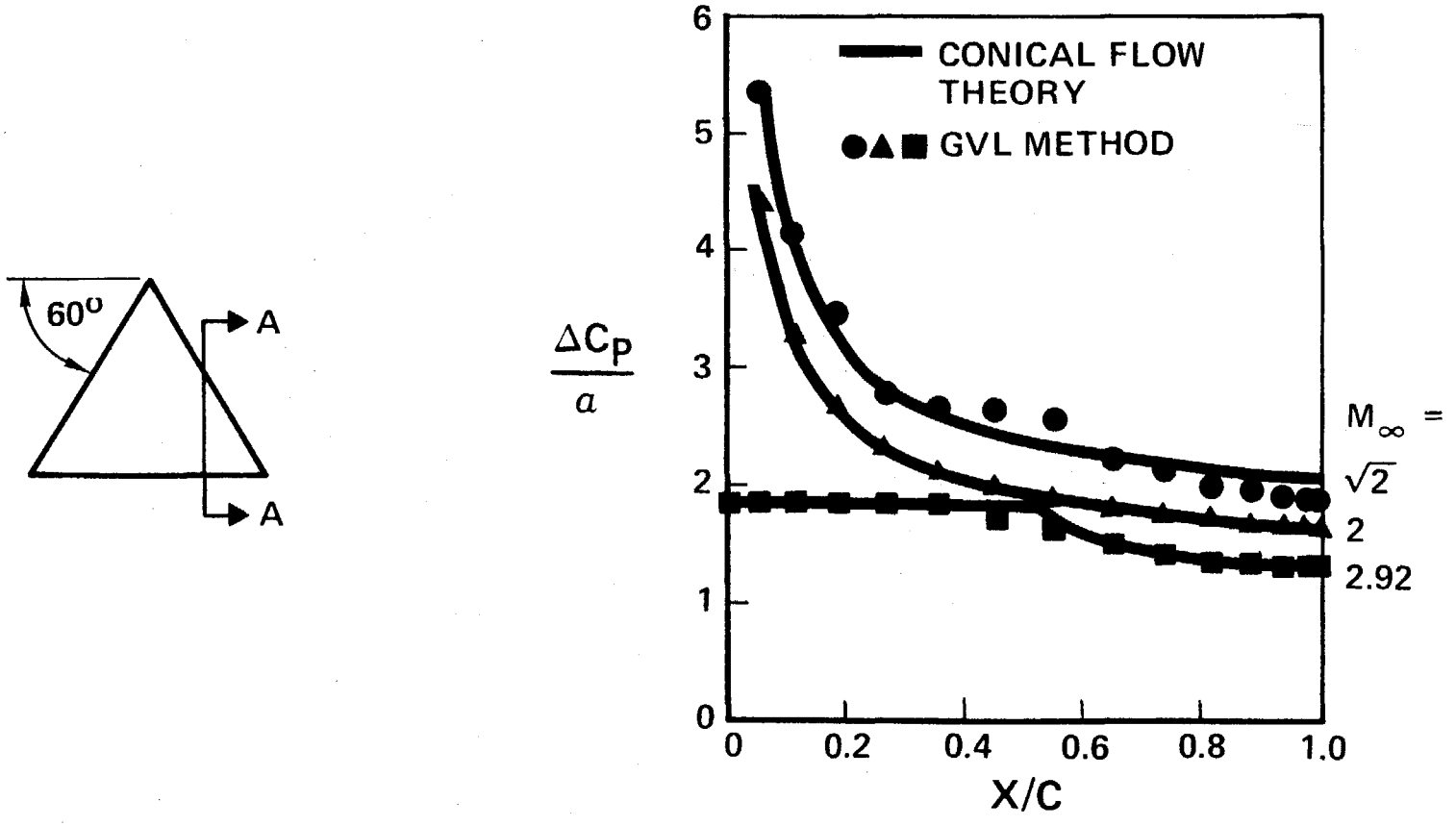

Figure 11.- Theoretical comparison of chordwise loading for delta wing.

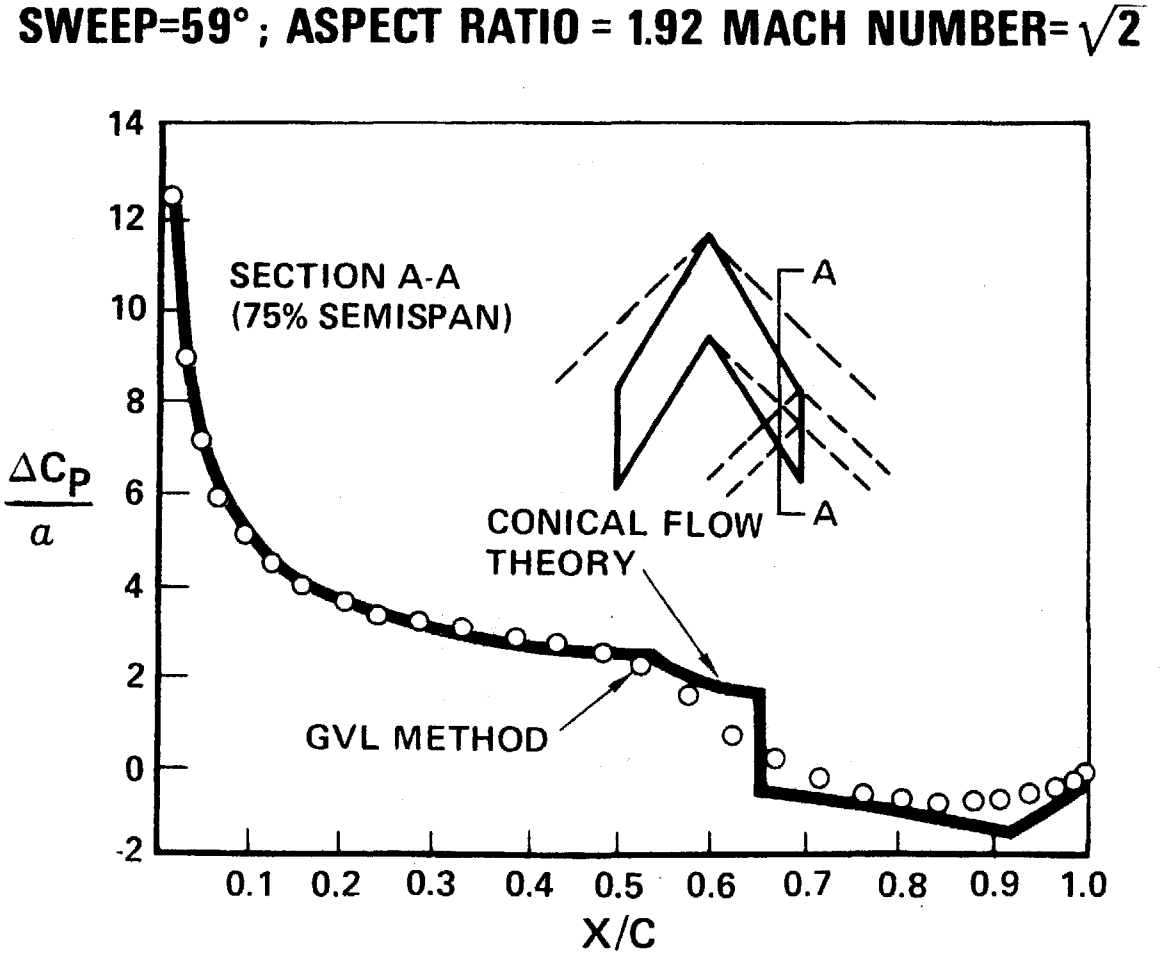

Figure 12.- Theoretical comparison of chordwise loading for sweptback rectangular wing.

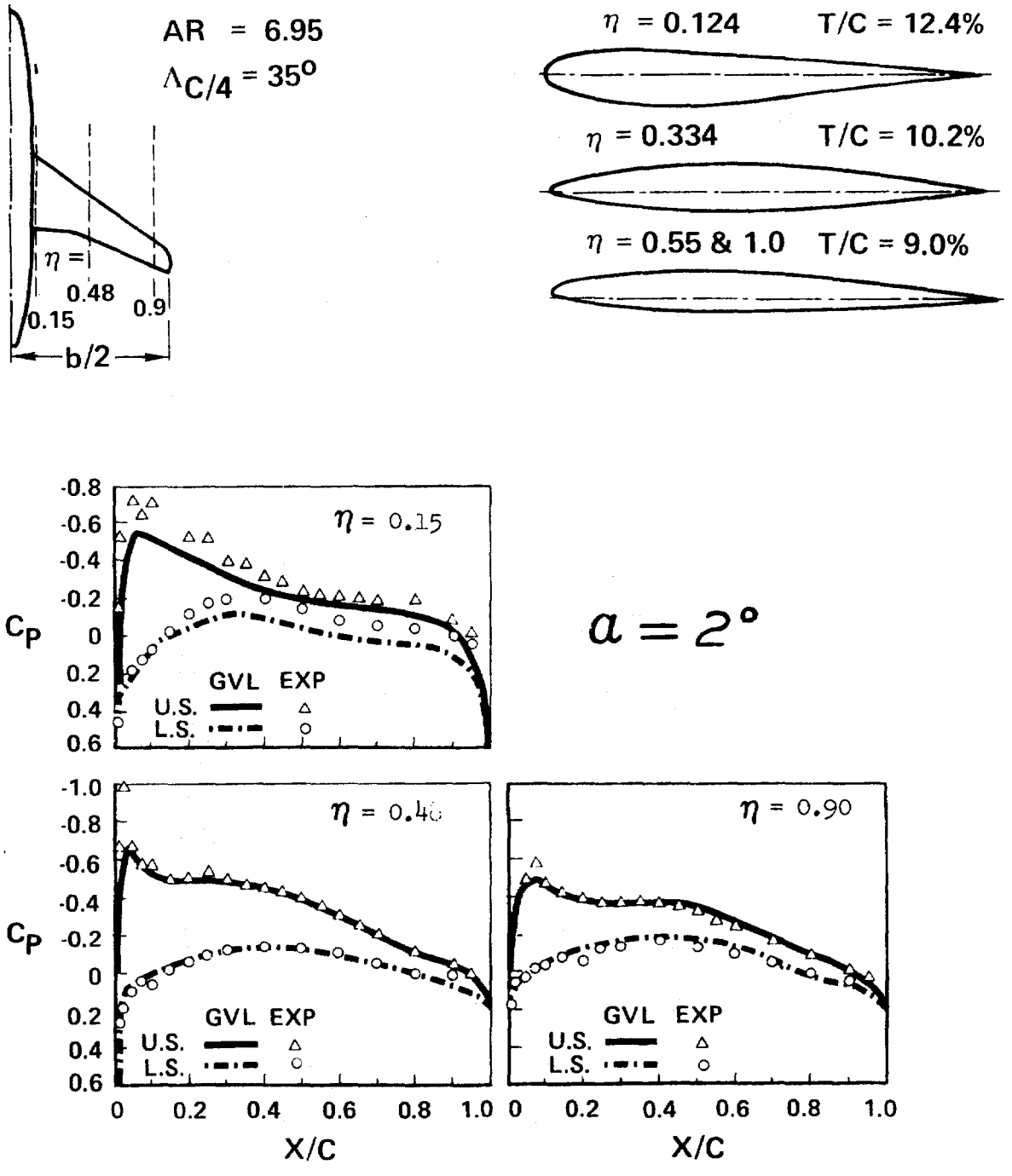

Figure 13.- Comparison with experimental pressure distribution on wing-body model at Mach = 0.5.

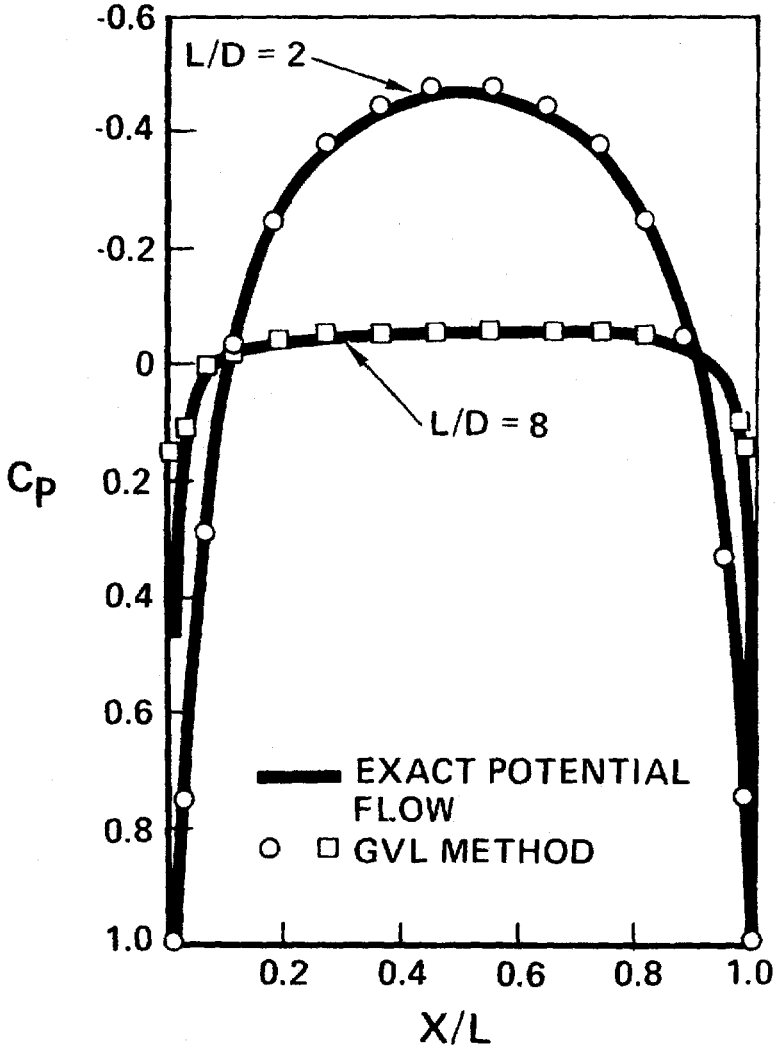

Figure 14.- Theoretical comparison of pressure distribution on ellipsoids at zero angle of attack in incompressible flow.

APPENDIX A

USER'S MANUAL
FOR
A GENERALIZED VORTEX LATTICE METHOD
FOR SUBSONIC AND SUPERSONIC FLOW APPLICATIONS

THE VORLAX COMPUTER PROGRAM

A computer program has been developed for the aerodynamic analysis and design of arbitrary aircraft configurations in subsonic and supersonic flow. This computer program, herein identified as VORLAX, has been codified in FORTRAN IV for use on the CDC 6600, the IBM 360, and the IBM 370 digital computer systems. A complete compilation and executed case in CDC FORTRAN IV is contained in Appendix B. Two auxiliary interface programs, treated in Appendices C and D, provide for input data transformation from NASA Wave Drag format (Reference 12) to VORLAX format (Appendix C) and for transformation from VORLAX to NASA Wave Drag format (Appendix D).

The VORLAX program is based on a generalized vortex lattice (GVL) method which extends the applicability of vortex lattice techniques to a broader range of problems than has heretofore been considered. In this program, the configuration is represented by a three-dimensional, generally nonplanar, vortex lattice; the basic element of the lattice is the skewed horseshoe vortex whose induced velocity formulas have been generalized for subsonic and supersonic flow. Thickness effects can be simulated by a double (biplanar or sandwich) lattice arrangement. Fusiform bodies can be modelled by a concentric cylindrical lattice of polygonal cross sections. The computational capabilities of the program include the following:

- Surface pressure or net load coefficient distribution.
- Aerodynamic force and moment coefficients.
- Surface warp (camber and twist) design in order to achieve input pressure distribution.
- Longitudinal/lateral stability derivatives.
- Ground and wall (wind tunnel interference) effects.
- Flow field survey.
- Symmetrical/asymmetrical configurations and/or flight conditions.

The limitations of the VORLAX program are characteristic of methods based on inviscid linearized potential flow theory, as follows:

- Attached flow.
- Small perturbation flow.
- Flow entirely subsonic or supersonic (no mixed transonic flow).
- Straight Mach lines.
- Rigid vortex wake.

In defining a configuration for the program input, a master frame of reference X- Y- Z- is assumed. The X-Z plane is the centerline plane, the Z axis directed upward, and the X-axis pointing in the downstream direction; the Y axis points to starboard. The origin of the system can be any convenient point in the X-Z plane. In general, the configuration can be made up of symmetrical and asymmetrical components, and in defining the symmetrical components only the starboard elements need be specified.

The configuration to be input is divided into a set of major panels; up to 20 of these panels can be input, symmetrical components being counted only once. For instance, a wing with straight leading and trailing edges, and with linear lofting between the root and tip, constitutes a major panel. Complex planforms, and nonlinear changes in twist and airfoil sections are described by defining more than one panel for a given wing. The computer program will then subdivide each major panel into a number of smaller elementary panels spaced chordwise and spanwise, i.e., a finer mesh lattice is generated internally. The chordwise and spanwise spacing is specified by the user, two options being available: (1) the semicircle or cosine distribution so well known in airfoil and wing theory, and (2) the equally spaced distribution.

Up to 2000 elementary panels can be used in the definition of a given configuration. Any consistent system of length and area dimensions can be used in the specification of the configuration length, but it is recommended that the system of units used be such that the largest length dimension does not require more than three digits to the left of the decimal point. Otherwise, significant digits may be lost in the output printout.

Wing thickness effects can be taken into account within the context of control surface theory. By control surface theory one means that the exact linearized theory is used to evaluate induced velocities along a given mean surface, known as the control surface, and these values enter into the computation of the boundary conditions which are satisfied at this control surface rather than at the actual boundary surface. The control surface equivalent of a typical two-dimensional airfoil is illustrated in figure A-1. The assumption inherent in control surface theory is that the induced velocities vary very little in the vicinity of the surface. Experience has shown that for the majority of practical configurations the loss in accuracy is negligible, and is more than compensated for by the increase in computational efficiency. Any wing-like component with thickness is then represented by a double set of panels, one for the upper surface and one for the lower surface as shown schematically in figure A-2.

All the swept horseshoe vortices, and their boundary condition control points, corresponding to a given surface, upper or lower, are located in a same plane. The upper and lower surface lattice planes are separated by a gap which represents the chordwise average of the airfoil thickness

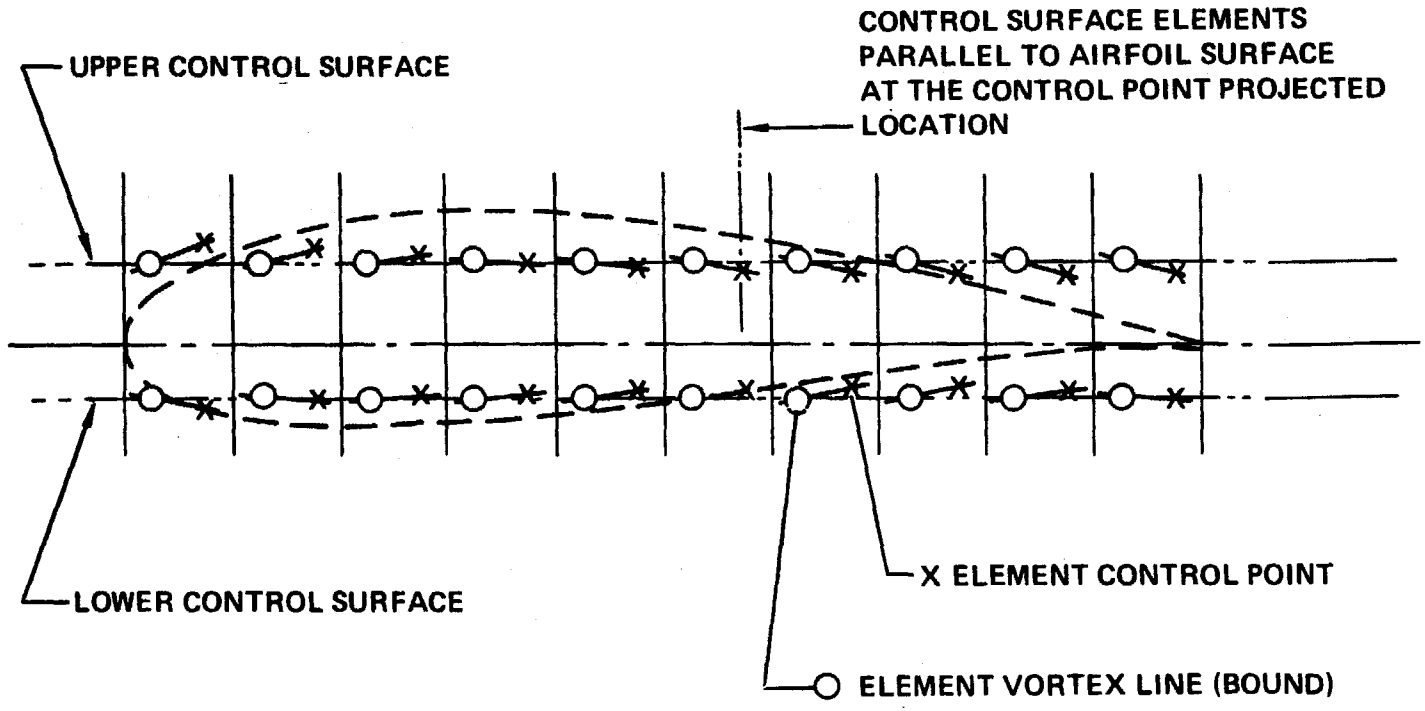

Figure A-1. - Control surface nomenclature

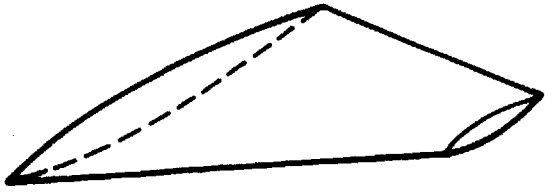

ACTUAL WING PANEL

BOUNDARY CONDITION: $\bar{w} \cdot \bar{n}' = \bar{v} \cdot \bar{n}' = -\bar{u}_\infty \cdot \bar{n}$; $\bar{n}' = m\bar{j} + n\bar{k}$

THIN PANEL LATTICE

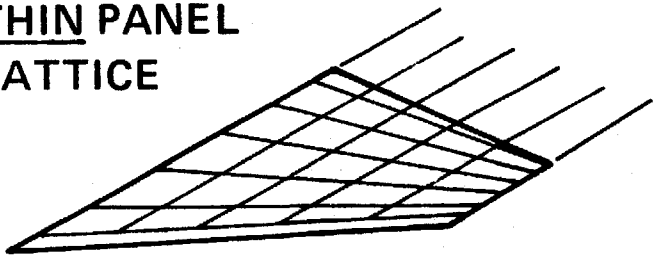

THICK PANEL LATTICE

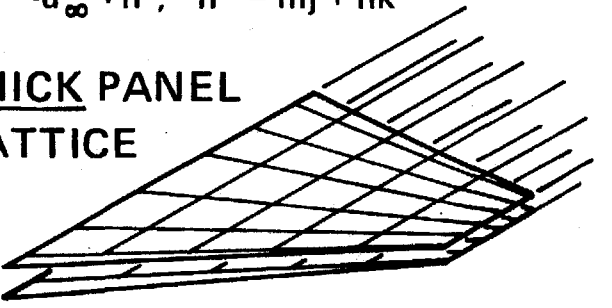

CHORDWISE DISTRIBUTION OF VORTEX LINES: $\frac{X_j^v - X_o}{C} = \frac{1}{2}\left\{1 - \cos\left(\pi \frac{2J-1}{2N}\right)\right\}$

CHORDWISE DISTRIBUTION OF B.C. CONTROL POINTS: $\frac{X_j^c - X_o}{C} = \frac{1}{2}\left\{1 - \cos\left(\pi \frac{J}{N}\right)\right\}$

Figure A-2. - Modeling of thick wing with horseshoe vortices

distribution. The results are not too sensitive to the magnitude of this gap; any value between one half to the full maximum chordwise thickness of the airfoil has been found to be adequate, the preferred value being two thirds of the maximum thickness. Furthermore, the gap can vary in the direction normal to the x-axis to allow for spanwise thickness taper. On the other hand, the chordwise distribution, or spacing, of the transverse elements of the horseshoe vortices have a significant influence on the accuracy of the computed surface pressure distribution. For greater accuracy, for a given chordwise number of horseshoe vortices, the transverse legs have to be longitudinally spaced according to the cosine distribution law

$$x_j^v - x_o = \frac{c}{2}\left[1 - \cos\left(\pi \frac{2J-1}{2N}\right)\right]$$

where $x_j^v - x_o$ represents the distance from the leading edge to the midpoint of the swept leg of the Jth horseshoe vortex, c is the length of the local chord running through the midpoints of a given chordwise strip, and N is the number of horseshoe vortices per strip. The chordwise control point location corresponding to this distribution of vortex elements is given by

$$x_J^C - x_o = \frac{c}{2}\left[1 - \cos\left(\pi \frac{J}{N}\right)\right]$$

The control points are located along the centerline, or midpoint line, of the chordwise strip (figure A-3).

The modeling of fusiform bodies with horseshoe vortices requires a special concentric vortex lattice if the simulation of the volume displacement effects, and the computation of the surface pressure distribution, are to be carried out. To define this lattice, it is necessary to consider first an auxiliary body, identical in cross-sectional shape and longitudinal area distribution to the actual body, with a straight baricentric line, i.e., without camber. The cross-sectional shape of this auxiliary body is then approximated by a polygon whose sides determine the transverse legs of the horseshoe vortices. The vertices of the polygon and the axis of the auxiliary body, which by definition is rectilinear (zero camber) and internal to all possible cross sections of the body, define a set of radial planes in which the bound trailing legs of the horseshoe vortices lie parallel to the axis (figure A-4). As the body cross section changes shape along its length, the corresponding polygon is allowed to change accordingly, but with the constraint that the polygonal vertices must always lie in the same set of radial planes. As in the case of the biplanar representation of thickness effects, cosine axial spacing should be used for the analysis of fusiform bodies. The effect of body camber is taken into account by independently specifying the camber of the baricentric axis of the body.

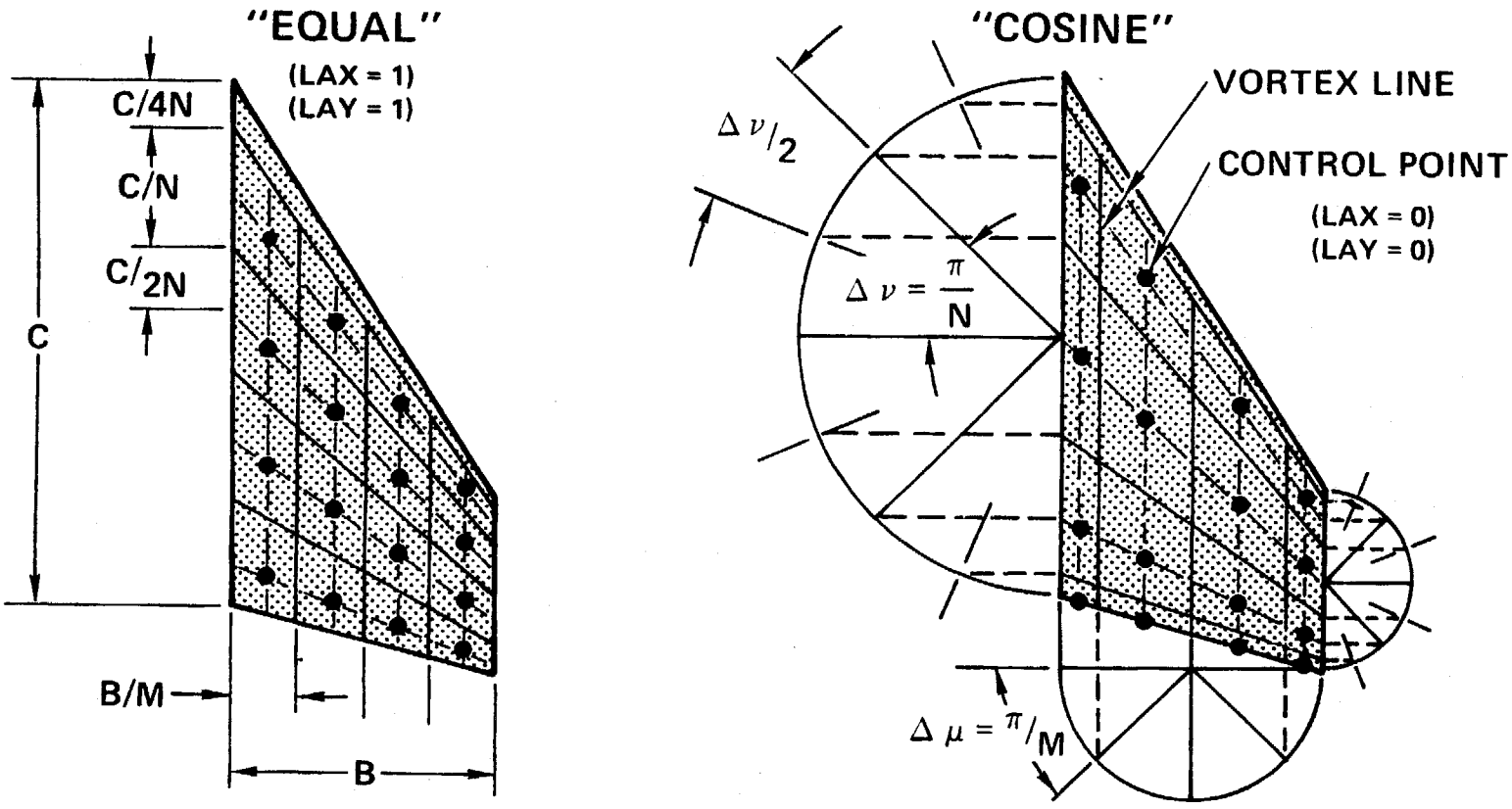

Figure A-3. - Vortex lattice collocation

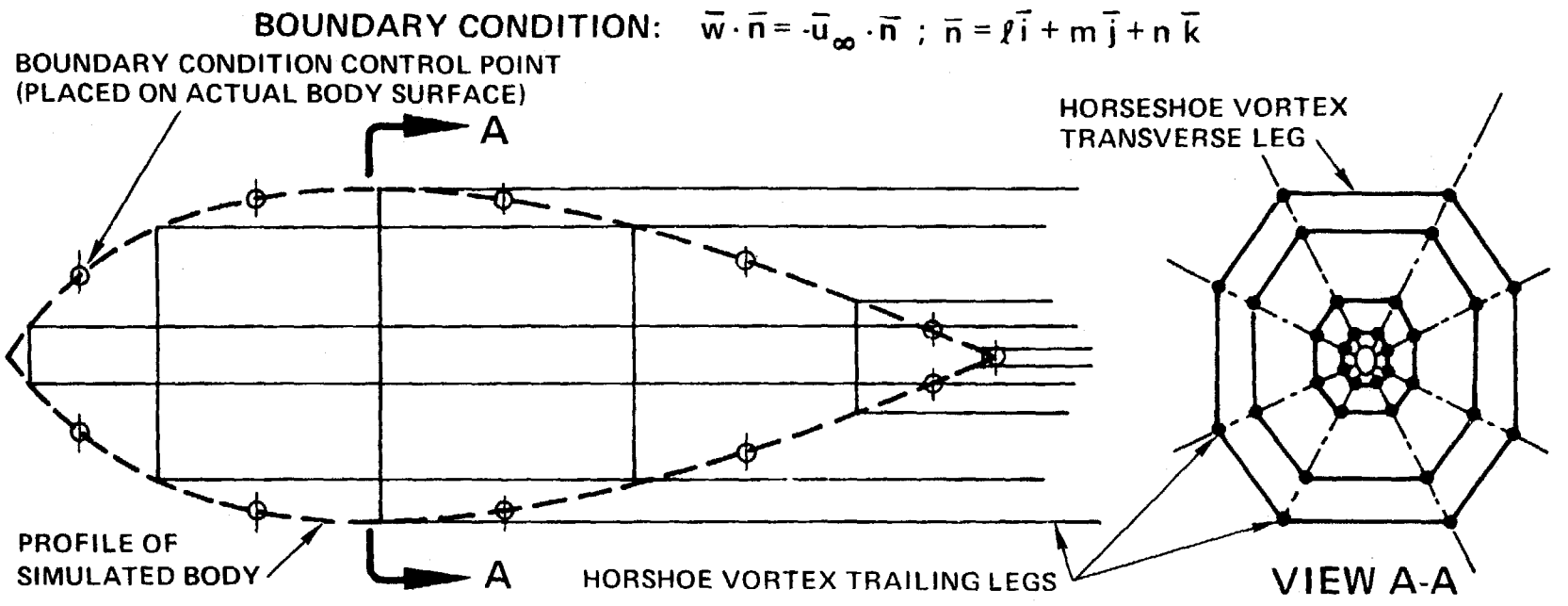

Figure A-4. - Modeling of fusiform body with horseshoe vortices

INPUT CARD IMAGE DESCRIPTION

The cards that constitute the input data deck are described in the following paragraphs. All format specifications are given in FORTRAN IV.

While some 19 cards are described, this does not mean that input for a case consists of 19 cards. Rather, these should be thought of as card types. Furthermore, not all card types will be included in a given case, those to be included or deleted being a function of some of the input values as shown in figure A-5.

CARD (1):	TITLE	In columns 1 through 80 write any alpha-numeric identification heading.
CARD (2):	ISØLV	Method to be used for solving the system of linear equations relating the boundary conditions to the vorticity strength, in integer format, in column 2. ISØLV = 0: Gauss-Seidel relaxation with accelerated convergence (under- or over-relaxation); ISØLV = 1: Purcell's vector orthogonalization method.
	LAX	Chordwise, or streamwise, spacing of vortices, integer quantity punched in column 12, LAX = 0: vortices are collocated at the percent chord (X/C) values determined by the cosine law $X/C - 0.5\,(1-\cos((2K-1)\pi/2N))$, where K varies between 1 and N, N being the number of chordwise vortices; LAX = 1: vortices are collocated according to the equally-spaced quarter-chord law $X/C = (4K-3)/(4N)$. The cosine law is recommended for greater accuracy for a given number of vortices.
	LAY	Spanwise, or lateral, spacing of vortices, integer quantity punched in column 22. LAY = 0: vortices are spaced at intervals (elementary vortex span) given by the cosine distribution law $\Delta b = b_p(\cos((J-1)\pi/M)-\cos(J\pi/M))/2$, where Δb is the vortex element span, b_p is the panel span, and J varies between 1 and M, M being the spanwise number of vortices in a given panel; LAY = 1: vortices are equally spaced along the panel span, i.e., $\Delta b = b_{p/M}$. The cosine spacing is recommended for enhanced accuracy, but

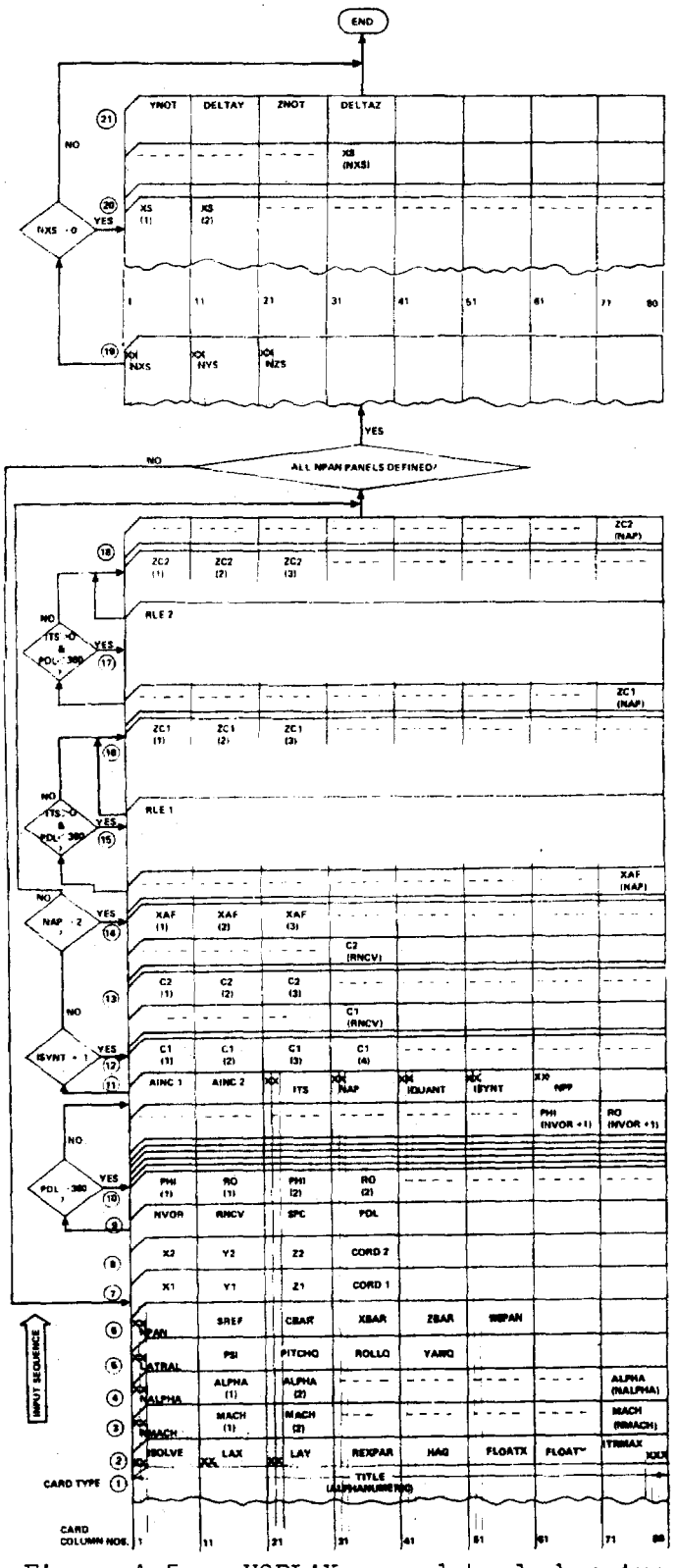

Figure A-5. - VORLAX case data deck setup

for most cases the difference in the results between cosine spanwise spacing and even spanwise spacing is negligible.

REXPAR — Over-relaxation parameter, in F10.0 format starting in column 31. This parameter is intended to accelerate the Gauss-Seidel relaxation process, and/or make it convergen when it might otherwise diverge. Blank, or zero, input, implies that the program will compute internally the optimum over-relaxation value. If a positive quantity between 0.01 and 0.99 is input, this becomes the value of the over-relaxation parameter that the program will use, the optimum value being overridden. If ISØLV = 1, this parameter is not used, and therefore, not a required input quantity.

HAG — Height above ground of the moment reference center, in F10.0 format starting in column 41. If it is punched equal to zero, or left blank, the height above the ground is infinity, i.e., no ground effect. If a quantity different than zero is input, then the ground effect will be computed by the method of images, the height being given by the input value, in consistent units.

FLØATX — Longitudinal vortex wake flotation factor, in F10.0 format, starting in column 51. If zero, or blank, then the trailing vortex legs being shed from the corresponding trailing edges, extend to infinity parallel to the X-Y plane. If a value different from zero is input, then the trailing vortex legs shed from the trailing edges form an angle α_V=FLØATX·ALPHA with the X-Y plane, where ALPHA is the freestream angle of attack. (See figure A-6)

FLØATY — Lateral vortex wake flotation factor, in F10.0 format, starting in column 61. If zero or blank, then the trailing vortex legs being shed from the corresponding trailing edges extend to infinity parallel to the X-Z plane. If a value different from zero is input, then the vortex legs shed from the trailing edges form an angle

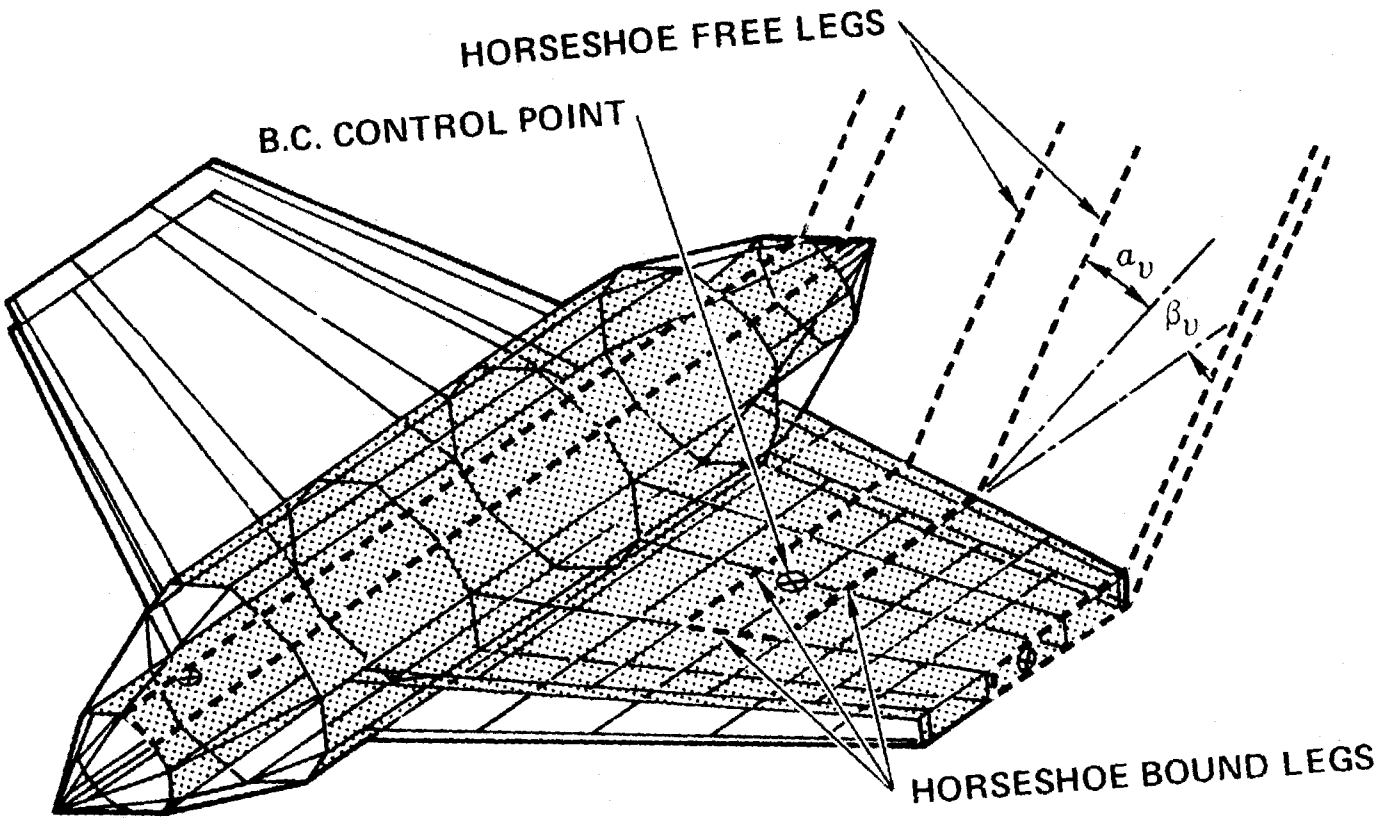

Figure A-6. Generalized vortex lattice model of wing body configuration

		β_v = FLØATY·BETA with the X-Z plan, where BETA is the freestream angle of slideslip (see figure A-6).
	ITRMAX	Maximum number of iterations allowed for the Gauss-Seidel relaxation method, in I3 format right-adjusted to column 80. If no value is input, the code will make ITRMAX = 99 by default. If ISØLV = 1, i.e., the vector orthogonalization solution is resorted to, then ITRMAX is not a required input.
CARD (3):	NMACH	Number of Mach numbers to be analyzed, in I2 format; i.e., integer value of NMACH in column 2. NMACH ≤ 7.
	MACH	Mach numbers in F10.0 format starting in column 11.
CARD (4):	NALPHA	Number of angles of attack in I2 format; i.e., integer value of NALPHA in column 2. NALPHA ≤ 7.
	ALPHA	Angles of attack in degrees in F10.0 format, starting in column 11.
CARD(5):	LATRAL	Asymmetric flight or configuration flag. 0 in column 2 = symmetric flight and symmetric configuration about the X-Z plane. 1 in column 2 = asymmetric flight and/or asymmetric configuration.
	PSI	Sideslip angle in degrees in F10.0 format starting in column 11. + = wind coming from left side of nose. Input 0. or blank when LATRAL is 0. Used to obtain static stability derivatives such as C_{n_β}, C_{y_β}, etc.
	PITCHQ	Pitch rate in degrees/second in F10.0 format starting in column 21. + = nose up pitch. Used to obtain dynamic stability derivatives such as Cm_q, C_{L_q}, etc. LATRAL may be 0 when PITCHQ is nonzero.
	RØLLQ	Roll rate in degrees/second in F10.0 format starting in column 31. + = left roll. Input 0. or blank when LATRAL is 0. Used to obtain dynamic stability derivatives such as C_{ℓ_p}, C_{n_p}, etc.

	YAWQ	Yaw rate in degrees/second in F10.0 format starting in column 41. + = left yaw or airstream component washing from left to right across nose of airplane. Input 0. or blank when LATRAL is 0. Used to obtain dynamic stability derivatives such as C_{n_r}, C_{y_r}, etc.
	VINF	Reference free stream velocity in F10.0 format starting in column 51. If no value is input, VINF is automatically set equal to 1.0 by the program. This parameter is only used when any of the angular rates is different from zero. It enters in the computation of the equivalent flow angle. For instance, if VINF = WSPAN/2 (wing semi-span) and ROLLQ = 5.73, then pb/2V = 0.1, and the rolling moment coefficient printed out by the program will be exactly one-tenth the value of the stability derivative C_{ℓ_p}. Likewise, if VINF = CBAR/2 (half the mean aerodynamic chord) and PITCHQ = 5.73, then the difference between the output pitching moment coefficient and the pitching moment coefficient for the case PITCHQ = 0. will be equal to one-tenth of the C_{m_q} derivative.
CARD (6):	NPAN	Number of major panels that will define the configuration, in I2 format; i.e., integer value of NPAN in columns 1-2 right adjusted to 2. NPAN $\leq$20.
	SREF	Reference area for force and moment coefficients, in F10.0 format starting in column 11.
	CBAR	Pitching moment coefficient reference length, in F10.0 format starting in column 21. Usually mean aerodynamic chord length.
	XBAR	Abscissa of moment reference point, in F10.0 format starting in column 31. X-coordinate in master frame of reference.
	ZBAR	Ordinate of moment reference point, in F10.0 format starting in column 41. Z-coordinate in master frame of reference.

	WSPAN	Total wing span in units consistent with SREF and CBAR, in F10.0 format starting in column 51. If left blank, a value of 2.0 will be assumed by the program.
CARD (7):	X1	X or longitudinal coordinate of the leading edge of one side of a major panel. Usually taken as the most inboard side in the case of wings. Input in F10.0 format starting in column 1.
	Y1	Y or lateral coordinate of leading edge of first side of a major panel. Input in F10.0 format starting in column 11.
	Z1	Z or vertical coordinate of leading edge of first side of a major panel. Input in F10.0 format starting in column 21.
	CØRD1	Chord length of first side of major panel measured from X1, Y1, Z1 above in the positive direction of, and parallel to, the X axis.
CARD (8):	X2	X or longitudinal coordinate of the leading edge of the second side of the major panel described on card (7). Usually taken as the most outboard side in the case of wings. In the case of a closed curved panel, e.g., a cylindrical segment representative of a nacelle, X2 would be identical to X1. Input in F10.0 format starting in column 1.
	Y2	Y or lateral coordinate of leading edge of second side of the major panel described on Card (7). Input in F10.0 format starting in column 11.
	Z2	Z or vertical coordinate of leading edge of second side of the major panel described on Card (7). Input in F10.0 format starting in column 21.
	CØRD2	Chord length of second side of major panel measured from X2, Y2, Z2 above in the positive direction of, and parallel to, the X axis.

Note: Columns 41-80 of cards (7) and (8) are not read. Thus, any information useful for identification purposes may be written there.

Note that the side edges 1 and 2 of a major panel, which have just been described by the input in cards (7) and (8), define the direction of the positive normal for that panel. This is determined by the feet-to-head direction for an observer standing on the panel looking upstream (down the negative X-axis) and with panel edge 1 to his left, and panel edge 2 to his right. In this analogy it is assumed that gravity is not a factor in that an observer could be standing on the bottom of a wing, for example, equally as easily as he might stand on top. In the case of curved panels, such as a nacelle component, the direction of the positive normal loses its meaning for the panel as a whole, but it is still applicable to each one of the longitudinal, or chordwise, strips that make up the major panel.

CARD (9)

NVØR — Number of spanwise elements or vortices that will be used to represent the panel, in F10.0 format starting in column 1. NVØR ≤100.0.

RNCV — Number of chordwise vortices that will be used to represent the panel, in F10.0 format starting in column 11. RNCV ≤50. The program, using NVØR and RNCV, will subdivide the panel under consideration into a grid of NVØR x RNCV swept horseshoe vortices collocated in accordance with the values of the LAX and LAY parameters. Note that chordwise and lateral distributions are independent, e.g., a cosine chordwise spacing (LAX=0) is compatible with equal spanwise distribution (LAY = 1), and vice versa. The corresponding control points at which the boundary conditions are satisfied are collocated according to the law $(X/C)_{control} = 0.5\ (1-\cos\ (K\pi/N))$, K varying between 1 and N, where N is the number of chordwise vortices, if LAX = 0. If LAX = 1, then the control points are placed at $(X/C)_{control} = (4K-1)/(4N)$, namely, according to the equally spaced three-quarter chord distribution. The spanwise location of the control points is always at the centerline of the elementary swept horseshoe vortices.

To determine the surface slope at each element control point, the program uses straight line element lofting between the two longitudinal, or butt line, edges of the major panel.

In addition to the above limitations to the values of NVØR and RNCV, if more than one major panel is used in the description of the configuration, the following should be observed:

$$\text{If LATRAL=0,} \quad \sum_{1}^{NPAN} \text{NVØR} \times \text{RNCV} \leq 2000$$

$$\text{If LATRAL=1,} \quad \sum_{1}^{NPAN} \text{NVØR} \times \text{RNCV} \times \text{IQUANT} \leq 2000$$

IQUANT being defined further down.

SPC — Leading edge suction multiplier, in F10.0 format starting in column 21. 0. = no suction. 1. = 100 percent leading edge suction. Nonzero values are recommended for all panels whose leading edges are wetted by the airstream. The program has the capability of computing the effects of free leading edge vorticity (leading edge vortex flows) by a localized application of the Polhamus analogy. This computation is triggered by inputting the SPC parameter as a negative quantity. When this is done, the sectional leading edge suction vector will be rotated normal to the camber surface at the leading edge, instead of the corresponding attached-flow tangential orientation, and the forces and moments will be computed using the rotated suction vector.

PDL — Planar/curved panel flag, in F10.0 format starting in column 31. 0. = planar major panel is to be described (including warped planar.) PDL = 999. (or >360.) = a curved major panel is to be described.

CARD (10): PHI — Polar coordinate angle of radius vector when defining the subpaneling of a curved major panel. Omit this card when PDL = 0. PHI is the angle measured from the horizontal in a plane parallel to the Y-Z plane. PHI = 0 coincides with a line parallel to and in the positive direction of the Y-axis. Positive values of PHI are measured counterclockwise when viewed from the rear of the aircraft.

PHI is input in F10.0 format starting in column 1. This and the subsequent input RØ constitute a polar coordinate pair. The number of pairs to be input = NVØR + 1. Four pairs per card may be input in F10.0 format starting in column 1. As many cards as necessary are used. While the location of the origin from which the polar angle, PHI, is arbitrary the first PHI, RØ polar coordinate pair must coincide with the Y1, Z1 rectangular coordinates input on Card (7). Likewise, the last input polar pair must coincide with the Y2, Z2 of Card (8).

RØ — Radius vector from arbitrary origin when defining the subpaneling of a curved major panel. Input in F10.0 format. Each RØ is part of a PHI, RØ polar coordinate pair.

CARD (11): AINC1 — Tangent of the angle subtended by major panel root chordline, or first edge (described in Card (7)), and the positive X-axis, in F10.0 format starting in column 1. Sign convention is determined by observing the edge 1 chordline and the X-axis from edge 2. The edge 1 chord is then rotated counterclockwise until it is parallel to the X-axis. If the angle rotated through is less than 90 degrees then the angle, and consequently its tangent, are considered positive. If it is greater than 90 degrees, then AINC1 is negative.

AINC2 — Tangent of the angle subtended by major panel tip chordline, or second edge (described in Card (8)), in F10.0 format starting in column 11. Sign convention is determined by observing edge 2 and the X-axis, looking in the direction from edge 2 toward edge 1. The edge 2 chord is then rotated counterclockwise until it is parallel to the X-axis. If the angle rotated through is less than 90 degrees, then the sign is positive; otherwise it is negative.

ITS — Surface flag input as a two place integer in columns 21 and 22, right-adjusted to column 22. ITS = 0 or blank indicates that the panel is considered as a lifting surface of zero thickness, i.e., both its upper and

lower surface are wetted by the external flow. ITS = 01 means that only the panel upper surface is wetted by the real external flow. ITS = -1 indicates that only the panel lower surface is wetted by the real external flow. A double panel setup can then be used to represent a wing-like component with non-zero thickness, as previously illustrated in Figure 2. Notice that the X1, Y1, Z1, X2, Y2, and Z2 values to be input correspond to the control surface plane, and not to the actual chordal plane. The results are not critically sensitive to the separation between the upper surface panel (ITS = 01) and the lower surface panel (ITS = -1), a separation of two thirds the thickness ratio of the airfoil being a good average value to use.

NAP — Number of percent chords or stations along the chord (CØRD1 and CØRD2) at which the camber, or surface, ordinates are to be input. Input as a two-place integer in columns 31 and 32, right-adjusted to column 32. Maximum value of NAP is 50. A NAP = 0, 1, or 2 will be interpreted as a flat wing and no subsequent camber cards will be expected. If ISYNT, on this same card, is to be input as 1, i.e., a design case, then NAP should be 0 or blank.

IQUANT — Symmetry flag with respect to X-Z plane input as an integer in column 42. IQUANT = 0 or 2 indicates there is a mirror image of the panel on the opposite side of the X-Z plane. IQUANT = 1 indicates the panel is unique to the side for which it is being input.

ISYNT — Design/analysis flag input as an integer in column 52. ISYNT = 0 or blank indicates that the panel has been defined geometrically and only analysis is to take place. ISYNT = 1 indicates that the panel camber is to be designed by the program to support a specified pressure distribution. If NAP on this same card was input >2, then ISYNT should be zero or blank.

	NPP	Nonplanar parameter, input as on integer in column 62. NPP = 0 indicates that all the vortex filaments representing a given surface lie in the cylindrical surface whose directrix is the leading edge of the panel, and whose generatrices are all parallel to the X-axis. NPP = 1 denotes that the transverse vortex. filaments are located on the actual body surface, but the bound trailing legs are parallel to the x-axis. This parameter affects the definition of ZC_1 and ZC_2 on cards 16 and 18.
CARD (12):	C1	Pressure coefficients along the first, or root, edge of major panel defined on Card (7). If ISYNT = 0, then this card is omitted. Units are dimensionless, $\Delta p/q$. Format is 8F10.0 starting in column 1 with as many cards as necessary to input RNCV values of C1. The desired values of the aerodynamic loading are defined at the chordwise location of the vortex lines. Thus, if LAX = 0, the corresponding X/C points follow the cosine distribution $(1-\cos((2K-1)\pi/2N))/2$; if LAX = 1, then the definition points are located by the law $(4K-3)/4N$. In the above expressions K ranges between 1 and N, N being equal to RNCV, the chordwise number of vortices.
CARD (13):	C2	Pressure coefficients along the second, or tip edge of major panel defined on card (8). If ISYNT = 0, then this card is omitted. Format is 8 F10.0 starting in column 1 with as many cards as required to input RNCV values of C1. Linear interpolation between corresponding values of C1 and C2 is used to obtain ΔC_p at intermediate spanwise values for the subpanels.
CARD (14):	XAF	Chord percent values at which camber, or surface ordinates will be supplied for the major panel, in 8F10.0 format starting in column 1 using as many cards as necessary to define NAP values of XAF. If NAP is 0, 1, or 2, then a flat uncambered surface is implied and this card is omitted. These chord percents

need not be equally spaced, but the same set applies to both the root and tip chords, or edges of the panel. Second order Lagrange or sliding parabola interpolation is used to interpolate between input XAF points to obtain the surface slope value at the control point of each subpanel.

For a panel representing the surface of a non-zero thickness airfoil or body, ITS $\neq$ 0, the Lagrange interpolation is modified to a fractional power (1/2) Lagrange method in the neighborhood of the leading edge. This allows the precise definition of the surface slopes at the control points for a blunt leading edge.

CARD (15): RLE1

Leading edge radius, in percent chord, of airfoil section at the first, or root, edge of panel, in F10.0 format between columns 1 and 10. This card exists only if ITS $\neq$ 0, PDL <360.0 and NAP >2, i.e., an airfoil with non-zero thickness is being simulated. Otherwise, it must be omitted.

CARD (16): ZC1

Camber ordinates or surface ordinates of root chord of the major panel described on Card (7) in units of percent chord, in 8F10.0 format, using as many cards as necessary to input NAP values, each corresponding to an XAF of the Card (14) series. Omit this card if NAP is 0, 1, or 2. If a lifting surface, such as a wing, is being simulated by a zero thickness panel then the ordinates of the wing camber line should be input here. If the wing thickness is being simulated by the sandwich or biplanar, method, i.e., a separate panel for upper and lower surfaces, then the surface ordinates for upper or lower should be input here. If a curved panel is being simulated (i.e., PDL >360.) and NPP = 0 then ordinates of the panel streamwise edge should be input. These might represent the mean line of a shaped cowl for a flow through nacelle, for example. In this simulation all shed vortices will lie in the same cylindrical surface determined by the leading edge of the curved panel and the X direction. If NPP = 1

and PDL > 360.0, the ZC1 array represents the camber of the body axis.

CARD (17): RLE2 — Leading edge radius, in percent chord, of airfoil section at the second, or tip, edge of panel, in F10.0 format between columns 1 and 10. This card exists only if ITS $\neq$ 0, PDL < 360.0 and NAP > 2, otherwise it must be omitted.

CARD (18): ZC2 — Camber ordinates, or surface ordinates of the second, or tip chord of the major panel, or area ratios of the major panel in 8F10.0 format, using as many cards as necessary to input NAP values, each corresponding to ar XAF of the Card (14) series. Omit this card if NAP is 0, 1, or 2. Linear spanwise interpolation is used to obtain intermediate values.

If a curved panel is being simulated (PDL > 360.) and NPP = 1 then area ratios in percent are expected here. These should represent the ratio of the cross sectional area of the closed polygonal surface being simulated at the XAF station under consideration divided by the area of the reference polygon times 100. Note that ZC2 is entered in percent where a value of 100 represents a section exactly the size of the reference polygon. Values greater or less than 100 are permitted down to and including 0. The reference polygon is that input via the PHI-RO pairs on Card 10. In this simulation it is presumed that all stations along the panel have the same shape as the reference polygon, and the transverse vortices are located on the actual body surface of the curved panel.

This concludes the input for the first major panel of the configuration. If there is more than one panel, then start over with Card (7) and work down to this point. Panels may be input in any sequence.

After the last panel is described, continue with Card (19).

CARD (19): NXS — Number of X-stations that will define the spatial flow field survey grid. NXS = 00 means no survey desired. Maximum value of NXS is 20. Input as a two-digit integer in columns 1 and 2, right-adjusted to column 2.

	NYS	Number of Y-stations that will define the butt line values of the survey grid. NYS = 00 for no survey. NYS and NZS (following) may be any positive integer subject to NXS x NYS x NZS $\leq$2000. Input as a two digit integer in columns 11 and 12.
	NZS	Number of Z-stations that will define the water line values of the survey grid. NZS = 00 for no survey. Input as a two digit integer in columns 21 and 22.
CARD (20):	XS	X station values for the spatial flow field grid. Omit this card if NXS=0. Input in 8F10.0 format starting in column 1, using as many cards as necessary to define NXS values.
CARD (21):	YNØT	Beginning of grid in the butt line direction. Input in F10.0 format starting in column 1. Omit this card if NXS = 0.
	DELTAY	Y-spacing of the grid. There will be NYS butt line planes equally spaced a distance DELTAY apart. Input in F10.0 format starting in column 11.
	ZNØT	Beginning of grid in the water line direction. Input in F10.0 format starting in column 21.
	DELTAZ	Z-spacing of the grid. There will be NZS water line planes equally spaced a distance DELTAZ apart. Input in F10.0 format starting in column 31.

This ends the input description for a single case.

Consecutive data sets or cases can be submitted at the same time. The program will always identify the presence of a new set by the corresponding title card (Card (1)).

The program output is processed by a standard 132 characters-per-line printer. The output from each configuration is preceded by a printout of the input data cards. This printout is not an exact image of the input deck; rather, it is the version of the deck as the code sees it, namely, the default value of an input parameter is printed if there is a corresponding blank in the input card. Also, data within a format field are lined up for clarity in identification, even though in the input deck such data may be arbitrarily located within its field. The input deck data is followed by a list of the major geometric parameters used by the program and generated from the input data deck. Next, the component and total force and moment coefficients are printed out for a given flow condition (Mach number, angle of attack, angle of sideslip, and rotational velocities). These are followed by a tabulation of the location of all the vortex elements, the pressure coefficients, the circulation strengths, and other ancillary information. If a flow field survey about the configuration has been requested, then the flow parameters (velocity components, flow angles, Mach number, and pressure ratios) at a series of field grid points will be listed. If other flow conditions have been analyzed, the same type of output will follow for each one of them, starting with the listing of the component and total force and moment coefficients. If other configurations have been input, then the output will continue with the listing of the corresponding input data deck, and so on. Rather than describing the output format in detail, a glossary of the output terms, arranged in sequential order of appearance, and a sample computer output, Table A-1, are presented.

I — Numbering index for major panel identification. For cases where LATRAL = 1, the I-number preceded by a double asterisk in the PANEL GEOMETRY list denotes that the panel is the mirror image (about the X-Z axis) of the panel with the same I-number but without asterisks.

XAPEX — =XI (see input terminology).

YAPEX — =Y1 (see input terminology).

ZAPEX — =Z1 (see input terminology).

PDC — =PDC (see input terminology).

LESWP — Sweep of the panel leading edge, in degrees. Positive for sweepback, negative for sweep forward.

CSTART — =CØRD1 (see input terminology).

TAPER — Panel taper ratio, CØRD2/CØRD1.

PSPAN	Panel span.
NVØR	=NVØR (see input terminology).
RNCV	=RNCV (see input terminology).
SPC	=SPC (see input terminology).
SURF	Panel surface area.
CN	Panel normal force coefficient, referenced to its own surface area.
CL	Panel lift coefficient, wind axes, referenced to its own surface area.
CY	Panel lateral force coefficient, wind axes, referenced to its own surface area.
CD	Panel drag coefficient, wind axes, referenced to its own surface area.
CT	Panel leading edge thrust coefficient, referenced to its own surface area.
CS	Panel leading edge suction coefficient referenced to its own surface area.
CM	Panel pitching moment about moment reference center divided by (freestream dynamic pressure X SURF), wind axes.
CRM	Panel rolling moment about moment reference center divided by (freestream dynamic pressure X SURF), wind axes.
CYM	Panel yawing moment about moment reference center divided by (freestream dynamic pressure X SURF), wind axes.
SREF	=SREF (see input terminology).
WSPAN	=WSPAN (see input terminology).
CBAR	=CBAR (see input terminology).
CLTØT	Total (summation over all panels) lift coefficient referenced to SREF.
CDTØT	Total pressure drag coefficient, referenced to SREF.
CYTØT	Total lateral force coefficient, wind axes, referenced to SREF.

CMTØT — Total pitching moment coefficient about moment reference center, wind axes, referenced to SREF and CBAR.

CRTØT — Total rolling moment coefficient about moment reference center, wind axes, referenced to SREF and WSPAN.

CNTØT — Total yawing moment coefficient about moment reference center, wind axes, referenced to SREF and WSPAN.

E — Oswald's efficiency factor.

S — Perimetral, or spanwise, index of vortex element.

C — Chordwise, or streamwise, index of vortex element, 1 denotes leading edge element, and C value equal to RNCV corresponds to the last, or trailing edge element.

X/C — Percent chord location of bound vortex line.

X, Y, Z — Coordinates of horseshoe vortex element centroid (center point of bound vortex line).

CHØRD — Local chord length.

SLØPE — Surface slope at boundary control point.

ITS — Flag which indicates type of panel surface (see input terminology). A zero value means that the panel is considered as a zero thickness lifting surface. A positive unit value (1) denotes that the panel is the upper surface of an airfoil-like element. A negative unit value (-1) corresponds to the lower surface. In the case of body-like components, 1 denotes the external, or wetted, surface. For a flow-through nacelle arrangement, 1 stands for the external surface, and -1 for the internal surface.

DCP — Local loading coefficient ($\Delta C_p = C_{p\ell} - C_{pu}$) if panel ITS = 0. If ITS $\neq$ 0, then DCP is the local pressure coefficient (C_p).

CNC — Sectional normal force coefficient times local chord.

CN — Sectional normal force coefficient.

DL — Local dihedral, in degrees.

CMT — Sectional pitching moment coefficient about local quarter chord.

GAMMA — Vortex element circulation strength, divided by freestream velocity.

ZC/C — If the design option is being invoked, the resulting surface warp is printed out instead of GAMMA. This surface warp is expressed in fraction of the local chord, and it includes both camber and twist.

CTC — Sectional thrust coefficient times local chord.

CDC — Sectional pressure drag coefficient times local chord.

ITRMAX — Maximum allowable number of relaxation cycles if Gauss-Seidel solution is used (see input terminology).

EPS — Tolerance, or minimum, iteration change for relaxation process.

ITER — Actual number of relaxation cycles.

BIG — Actual iteration change for relaxation process. Relaxation will stop when BIG ≤ EPS, or when ITER = ITRMAX.

If a flow field survey about the configuration has been requested (NXS > 0 in the input deck, see input description), then the following parameters will also be output as part of this survey:

X, Y, Z — Coordinates of the survey grid points (not to be confused with the X, Y, Z coordinates of the vortex centroids previously described), referenced to the configuration master coordinate frame. The X, Y, Z coordinates are determined by the XS, YNOT, DELTAY, ZNOT, DELTAZ input values (see input terminology).

U — Dimensionless velocity (freestream velocity at infinity assumed to be unity) along the X-direction (body axes).

V — Dimensionless velocity along the Y-direction (body axes).

W — Dimensionless velocity along the Z-direction (body axes).

EPSLØN — Upwash angle in degrees. this angle is measured with respect to the X-axis in a plane parallel to the X-Z plane.

SIGMA — Sidewash angle in degrees. This angle is measured with respect to the X-axis in a plane parallel to the X-Y plane.

CP — Local field pressure coefficient ($CP = (P_{static}-P_{inf})/q_{inf}$).

MLOC — Local Mach number.

P/PTØT — Local static-to-total pressure ratio for isentropic flow.

P/PINF — Local to-freestream static pressure ratio for isentropic flow.